# Spatial-temporal heterogeneity and driving factors of water yield services in Citarum river basin unit, West Java, Indonesia

Irmadi Nahib*, Wiwin Ambarwulan, Dewayany Sutrisno, Mulyanto Darmawan, Yatin Suwarno, Ati Rahadiati, Jaka Suryanta, Yosef Prihanto, Aninda W Rudiastuti, Yustisi Lumban Gaol

Research Center for Geospatial, Research Organization for Earth Sciences and Maritime, National Research and Innovation Agency, Cibinong Science Center, Jl. Raya Jakarta-Bogor Km 46, Cibinong 16911, Indonesia

*Corresponding author's e-mail: irmnahib@gmail.com

**Abstract:** Many countries, including Indonesia, face severe water scarcity and groundwater depletion. Monitoring and evaluation of water resources need to be done. In addition, it is also necessary to improve the method of calculating water, which was initially based on a biophysical approach, replaced by a socio-ecological approach. Water yields were estimated using the Integrated Valuation of Ecosystem Services and Trade-offs (InVEST) model. The Ordinary Least Square (OLS) and geographic weighted regression (GWR) methods were used to identify and analyze socio-ecological variables for changes in water yields. The purpose of this study was: (1) to analyze the spatial and temporal changes in water yield from 2000 to 2018 in the Citarum River Basin Unit (Citarum RBU) using the InVEST model, and (2) to identify socio-ecological variables as driving factors for changes in water yields using the OLS and GWR methods. The findings revealed the overall annual water yield decreased from 16.64 billion $m^3$ $year^{-1}$ in the year 2000 to 12.16 billion $m^3$ $year^{-1}$ in 2018; it was about 4.48 billion $m^3$ (26.91%). The socio-ecological variables in water yields in the Citarum RBU show that climate and socio-economic characteristics contributed 6% and 44%, respectively. Land use/Land cover (LU/LC) and land configuration contribution fell by 20% and 40%, respectively. The main factors underlying the recent changes in water yields include average rainfall, pure dry agriculture, and bare land at 28.53%, 27.73%, and 15.08% for the biophysical model, while 30.28%, 23.77%, and 10.24% for the socio-ecological model, respectively. However, the social-ecological model demonstrated an increase in the contribution rate of climate and socio-economic factors and vice versa for the land use and landscape contribution rate. This circumstance demonstrates that the socio-ecological model is more comprehensive than the biophysical one for evaluating water scarcity.

## Introduction

Population growth has an impact on increasing water consumption (directly), at the same time increasing food production and consumption (indirect water consumption). In the perception of water management, we must take into account the fact that the world is developing very dynamically, the world population is continuously increasing, and thus the amount of water consumption is also increasing, while the amount of water per capita is continuously decreasing (Nie et al. 2019).

Water demand is expected to increase in all production sectors (WWAP. 2021), while the world is expected to witness a shortage of global water of 40% by 2030 in the business--as-usual climate scenario (Young and Esau 2013). Scarcity of water and groundwater depletion are major issues in many countries (Figueroa et al. 2020).

Indonesia's total renewable water resources in 2017 were 2,019 billion $m^3$ $year^{-1}$. Meanwhile, the total water demand is around 222.6 billion $m^3$ $year^{-1}$ (Worldmeter), and water resources per capita 7,648 $m^3$ $person^{-1}$ $year^{-1}$. Based on a national-level climate risk study by (Suroso et al. 2010, Sriyanti 2009), it was found that one area with a strong likelihood of water scarcity is the Java-Bali region (the water deficits, especially in several locations in the north and south of West Java).

One of the focus areas for the evaluation of climate risk is the Citarum RBU, West Java. The Citarum RBU ecosystem services must understand hydrological conditions by estimating elements affecting water yield. The potential availability of water in the Citarum river area in 2017 was 1.29 billion $m^3$

year$^{-1}$, while its utilization has only reached 7.65 billion m$^3$ year$^{-1}$ (Kementerian Pekerjaan Umum 2016).

Several factors affect the ecosystem services of a watershed (i.e., water yield); however, climate change and land use are significant determinants of ecological processes and ecosystem services (Pei et al. 2022). In its development, the approach based on biophysics has begun to be replaced with socio-ecological, namely biophysical factors plus social factors. The socio-ecological system is closely related between the community and the ecosystem (Francis and Bekera 2014). Glaser et al. 2008 defined a socio-ecological system (SES) consisting of a bio-geo-physical unit and associated social actors and institutions. SES are adaptive and complex and are limited by spatial boundaries.

The study on water yields in Poland, which analyzed the assessment of changes in water yields due to climate change, was carried out by (Kubiak-Wójcicka and Machul 2020, Borowski 2020, Sawicka et al. 2022, Szarek-Gwiazda and Gwiazda 2022, Borowski 2020, Zemełka 2019). In contrast, the relationship between water and land use can be explained by previous research (Dinka and Chaka 2019, Ambarwulan et al. 2021, Szwagrzyk, et al. 2018, Bucała-Hrabia 2018, Muhammed et al. 2021).

Climate change impact (an increase in air temperature per decade) caused higher evaporation and depletion of water resources. As a result, there was a decreasing tendency in the flow of the two major rivers (the Vistula and Oder) in Poland, which determined the size of Poland's water resources (Kubiak-Wójcicka and Machula 2020). Sawicka et al. 2022 explained that the impact of the rise in average temperature in April–May and June–July in Southeastern Poland, the potato yield was expected to escalate, assuming that the temperature escalation would be accompanied by a rise in rainfall during the period 2000 to 2019.

Meanwhile, the research of Barbieri et al. (2021) on Central Italy's carbonate aquifers shows that the impacts of climate change indicate that groundwater is more resilient than surface water. Climate change has the potential to impact groundwater quality by decreasing groundwater infiltration and enhancing anthropogenic stresses, negatively exacerbating water quality trends. According to Szarek-Gwiazda and Gwiazda (2022), climate change (from prolonged droughts to heavy rains) can significantly alter river flow regimes. The temperature and nutrient concentration in southern Poland's medium-sized mountain rivers are determined by the hydrological conditions of the year. The conductivity value and the amount of $NO_{3-}$ and $P_{-tot}$ in the water above the dam depend on how fast the water moves.

An rise in the frequency and intensity of precipitation in many parts of Europe (including Poland) will result in severe and frequent flooding. However, in other parts of Europe, including southern Europe, higher temperatures and less rainfall mean many areas could be affected by drought (Borowski 2020). Zemełka (2019) states that trends in land use change (conversion of agricultural areas into housing structures and services) influence the aquatic environment's pollution, ecological balance (decrease in the number of living organisms and biodiversity), as well as deterioration and quantitative changes in water quality.

The impact of changes in land use/land cover dynamics (LU/LC) (changes in vegetated natural areas for agriculture, grazing, and other land uses) in the watershed affects the hydrological process in the watershed by disturbing the ecological and environmental properties of the watershed, causing an increase in surface water and the formation of areas prone to erosion (Dinka and Chaka 2019, Bucała-Hrabia 2018), road density as a material and water transfer route to the Bucała-Hrabia channel (2018) and has an impact on land degradation (Ambarwulan et al. 2021). It also has a significant influence against flood risk because it reduces the effect on peak flood discharge (Szwagrzyk et al. 2018).

Referring to the research of Muhammed et al. (2021), the forest cover and rainfall rate relationship with water yield assessed on a global scale showed a relatively high correlation coefficient. In the rainy season, regional watershed deforestation causes a significant rise in discharge and flooding. On the other hand, it exacerbates the dry season flow.

One technique for monitoring and evaluating water yield was InVEST Model. The InVEST model is widely used, and it has been shown to be especially useful for strengthening ecosystem services like water yield (Yang et al. 2020). Sensitivity analysis of the InVEST model for water yield was carried out in a number of river basin areas, including the China watershed (Pei et al. 2022) and also in several locations in Indonesia (Nahib et al. 2021, Yudistiro et al. 2019, Siswanto and Francés 2019). Meanwhile, a study of water supply and demand in the Citarum watershed has also been carried out. The results show an inconsistency between water supply and demand caused by changes in the LU/LC due to human activities (Nahib et al. 2023).

Many countries, including Indonesia, are experiencing severe water scarcity and groundwater depletion. Monitoring and evaluation of water resources need to be done. Few studies examine the impact of changes in water yields on local scale watersheds in tropical Indonesia using a socio-ecological approach. Therefore, it is necessary to develop and improve a socio-ecological approach, to replace the biophysical approach. In the initial stage, applying socio-ecology in water resources for the tropical watershed level needs to choose the correct variables, namely landscape, and social integration. The method of determining the selection of variables as a driving factor for changes in water yields uses the OLS and GWR methods.

This study is aimed: (1) to analyze the temporal and spatial changes in water yield from 2000 to 2018 in the Citarum RBU using the InVEST model, and (2) to identify socio-ecological variables as driving factors for changes in water yields using the OLS and GWR methods. The results of this study are expected to be beneficial for decision-makers and environmental experts to manage watersheds sustainably.

## Materials and Methods

### *Study Area*

The research was carried out in the Citarum RBU, composed of 19 sub-watersheds situated in West Java Province, Indonesia (Figure 1).

The Citarum River (297 km) is the main river in this study area and has three major dams (Cirata, Saguling, and Jatiluhur) used for agriculture, electricity, and freshwater for the people who live in several regencies in West Java. The

Citarum river meets 80% of Jakarta's freshwater requirements. The Citarum watershed covers an area of 11,317 km$^2$ that encompasses 13 regencies. Geographically, the watershed is located at 7°19'–6°24' S and 106°51'36"–107°51' E. The Citarum RBU is situated in a humid tropical region with an average rainfall of 2,358 mm. Temperature in the lowlands is averaged around 27°C, while in the upstream part of the river in the highlands/mountains, the minimum air temperature is averaged at 15.3°C. Morphological conditions can be found in a wide range of environments, including volcanic edifices and hillsides. In addition, the highlands upstream of the Citarum tributary range in elevation from 750 to 2,300 meters above sea level, with slopes varying from 5 to 15% at the foot, 15 to 30% on the mountain slope, and 30 to 90% at the apex, whereas the plains upstream are morphologically formed by volcanic edifices with mild relief (Sholeh et al. 2018, BBWS Citarum Ciliwung).

The new paradigm in water resources management tries to describe watersheds as an integrated ecological system, and encourages stakeholders to pay attention to social and environmental aspects (Hasan 2011). The Citarum River which is located in West Java Province has very strategic natural resource potential. Environmental surroundings and water availability along the Citarum River, on the other hand, have deteriorated significantly over the last 20 years. This event is due to socio-ecological changes (climate, landscape configuration, land use, and socio-economic changes).

Infiltration is restricted to liquid water and more accurately describes the physical phenomena by which rain tries to enter the soil (Horton 1993). Infiltration greatly affects variations in surface runoff in addition to rainfall intensity, soil water content, and watershed size and slope.

### Dataset and Data Preparation
#### Calculating Water Yield using the InVEST Model
Table 1 shows remote sensing data as well as a variety of secondary data. Data were processed using the InVEST Model, geographic information system (GIS) technique, and R Studio.

As input for InVEST, the input data was transformed into raster data format with a spatial resolution of 30 m and referred to the WGS84 datum.

#### Water Yield Change's Driving Factors
This study considered four factors, referring to Zhang et al. (2021), i.e., climate, landscape configuration, socio-economic variables and land use (Table 2).

Land-use, climate, and socio-economic factors were considered as grid data and summarized using zonal statistics at the sub-watershed level. Referring to the previous study by Bin et al. (2018), five landscape-level metrics were chosen for
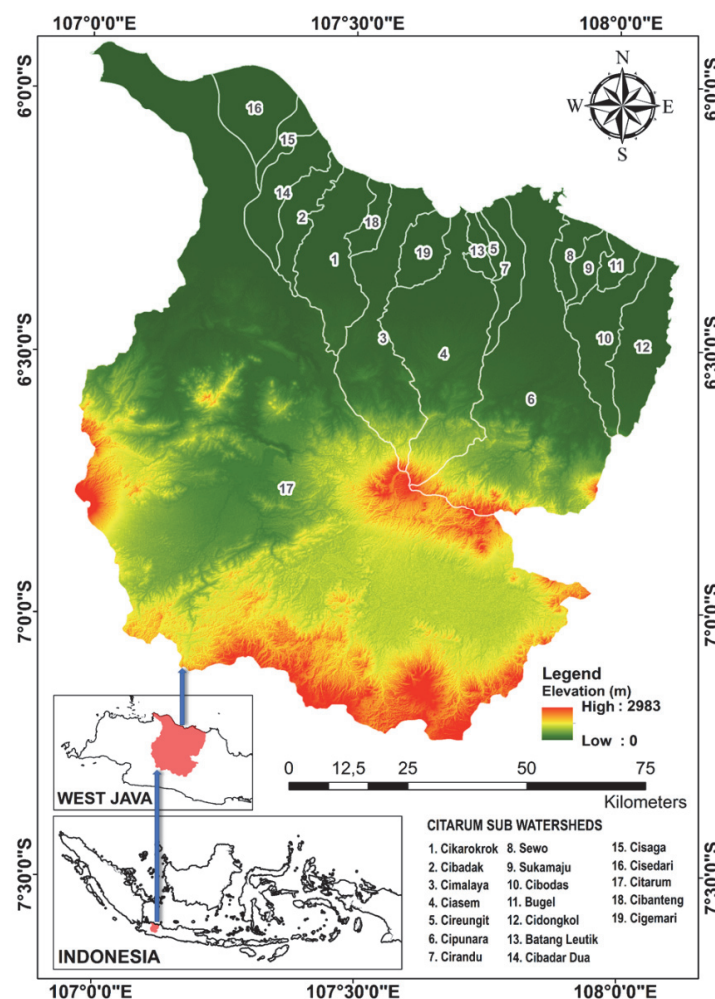


**Fig. 1.** Location and topography of Citarum RBU in West Java, Indonesia

each of the 19 sub-watersheds. To calculate landscape metrics, we used Fragstats 4.2 software.

## Methods

This research was divided into two stages (see Figure 3): at the first stage, The InVEST model was used to determine water yield and, at the second stage, socio-ecological variables were identified as the driving factors for changes in water yields.

The first stage of activity was carried out to answer the first objective, namely (i) calculating changes in water yields from the RBU Citarum from 2000, 2012, and 2018, (ii) simulating and analyzing variations in LU/LC and climate change in water yields from 2000–2012 and 2012–2018.

Water yield data (2000, 2012, and 2018) were validated with water yield data published by Geospatial Information Agency (BIG). The data from the modeled and actual water results were paired according to the location of the watershed/sub-basin. Furthermore, the paired data were analyzed using a linear regression model. To validate the model, root mean square error (RMSE), Pearson correlation (r), and the coefficient of determination ($R^2$) were calculated and used as a reference.

Water yield change data (the treatment result in the first stage) were used as the dependent variable (Yi). Meanwhile, as the independent variable (Xi), 20 variables were used (consisting of 3 climate variables, nine land use variables, five variable landscape configurations, and three socio-economic variables), as presented in Table 2. Furthermore, the dependent variable data and independent variables were paired with linear regression analysis to predict whether there was a relationship between the independent variables and changes in water yield. The analysis was carried out with the help of R Studio. This analysis was carried out using biophysical and socio-ecological models (by adding the integration of landscape variables to socio variables). The significance of each interaction model was compared, whether it strengthens or reduces changes in water yield. The results of the OLS model obtained a standard beta coefficient with a significant level, and the contribution rate of each variable to change in water yield.

The dependent and independent variables produced by the OLS model were then analyzed using the GWR approach to determine whether the model is global or local. Finally, the GWR Model could explain the site-specific and more detailed role of related factors in influencing changes in water yields.

**Table 1.** The data set used in this research

| Type of Dataset | Data Sources | Processing | Data Layout |
|---|---|---|---|
| LU/LC maps (2000, 2012, 2018 Land-use maps | Ministry of Environment and Forestry; US Geological Survey, http://www.usgs.govUSGS path/row122-121/64 | Converting Polygon to raster Extraction and reclassification Normalized Difference Vegetation Index (NDVI) | Raster data with a spatial resolution of 30 m |
| Rainfall and temperature | The National Bureau of Meteorology, Climatology, and Geophysics; Citarum Ciliwung River Basin Center; PT. Jasa Tirta II | Numerical/Table Data, with location coordinates a spline interpolation technique | Raster data with a spatial resolution of 30 m |
| Evapotranspiration map | WorldClim (https://worldclim.org/data/index.html) | a spline interpolation technique | Raster data with a spatial resolution of 30 m |
| Soil texture, organic matter content, and effective rooting depth Soil type data | Citarum Ciliwung River Basin Center | Extraction and resampling, convertion poligon to raster | Raster data with a spatial resolution of 30 m |
| Watershed boundaries | Citarum Ciliwung River Basin Center | Digital watershed atlas of natural resources | Vector |
| Biophysical | | | CSV |

**Table 2.** Description of potential driving factors investigated in this study

| Types | Factors |
|---|---|
| Climatic | (Average precipitation (mm), Average Evapotranspiration (mm), Average temperature (°C) |
| Land-use | Virgin Forest (%), Plantation Forest (%), Shrub (%),Estate Crops Plantation (%), Settlement Area (%), Bare land (%), Pure Dry Agriculture (%), Mixed Dry Agriculture (%), Paddy Field (%), Fishpond (%)*, Lake (%)*, Airport (%)* |
| Landscape configuration | Mean Patch Size (AREA_MN), Largest Patch Index (LPI), Aggregation Index (AI), Contagion (CONTAG), Mean Fractal Dimension Index (FRAC_MN) |
| Socio-economic** | Total GDP (IDR), GDP per capita (IDR/person), Total population (person) |

 * not included in the driving factor because there is only one sub-basin.
** The source of socio-economic data: the Central Bureau of Statistics of the Republic of Indonesia.

The results of the OLS model were a standard beta coefficient with a significant level and the level of contribution of each variable to changes in water yield.

In this study, both adaptive and fixed kernels were used to compute the bandwidth. The models from OLS, fixed GWR (FGWR), and adaptive GWR (AGWR) were compared, and their qualities were assessed in terms of the coefficient of correlation (r) and the residual sum of squares (RSS).

### Calculating Water Yield using the InVEST Model

For this research, the data source come from custodians. Watershed and sub-watershed boundaries, LU/LC maps, rainfall (mm), plant available water content (PAWC) percentage, soil depth (mm), and average yearly evapotranspiration potential (mm) are among the data used. The input data was all converted to raster. Among the data used are rainfall (mm), watershed and sub-watershed boundaries, LU/LC maps, average yearly

evapotranspiration potential (mm), soil depth (mm), and plant available water content (PAWC) percentage. All of the input data was converted to raster.

**Land use/Land cover (LU/LC).** The year 2000 was selected as the initial year based on the management of the Citarum RBU, stating that a paradigm shift and broadly comprehensive data availability had been established. When a six-year period is chosen, alterations in the forest (woody plants) in Landsat imagery can be effectively identified. All LU/LC data were divided into 12 categories: virgin forest, shrub, planned forest, settlement area, estate crops plantation, pure dry agriculture, bare land, paddy field, mixed dry agriculture, lake, fishpond, and airport.

InVEST requires information about LU/LC and the corresponding code, crop coefficient (Kc), and root depth. For land with no vegetation cover, root depth information is not required (Sharp et al. 2015). The vegetated LU/LC class was
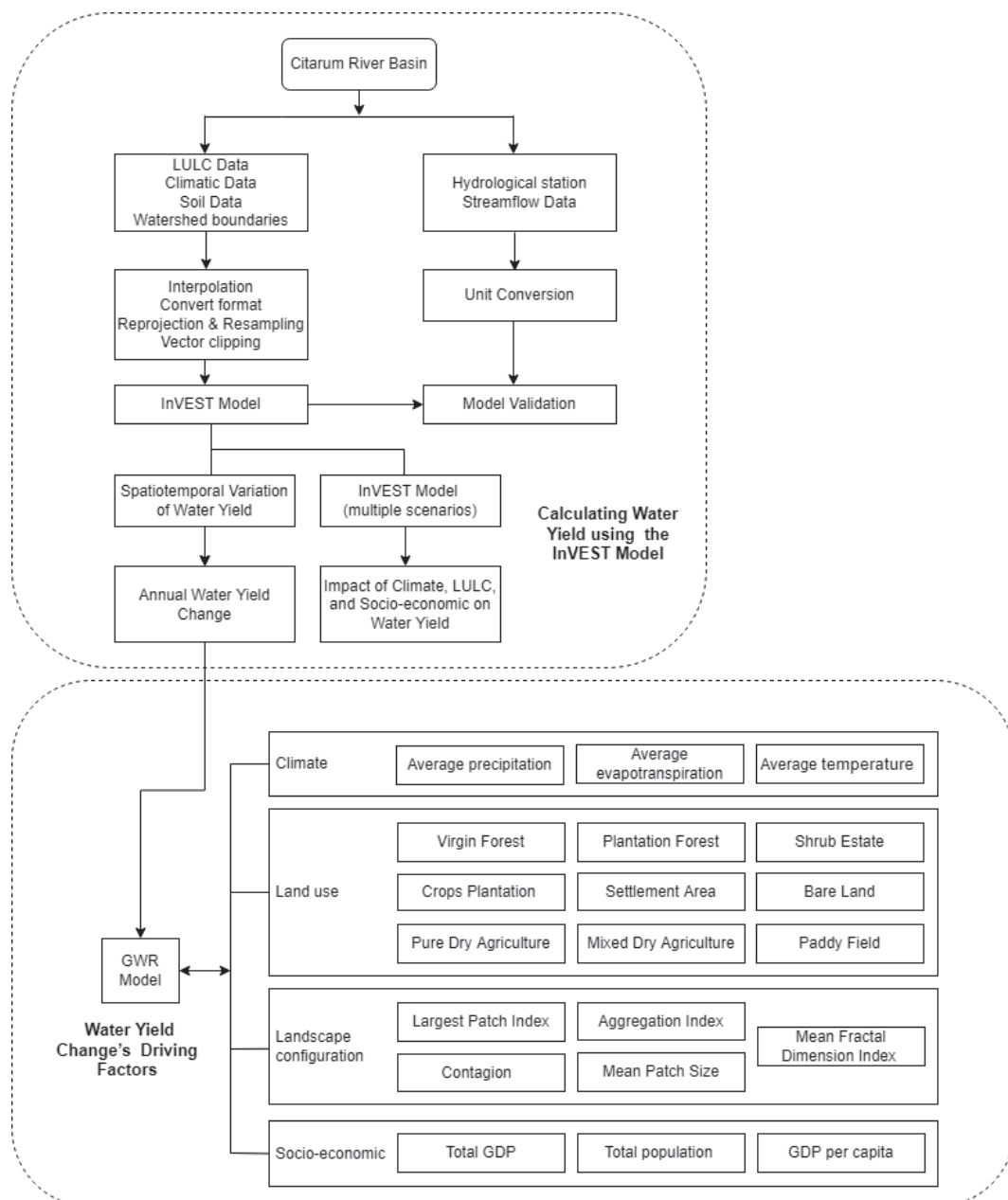


**Fig. 2.** Research flowchart

assigned a value of one in this study, while the non-vegetated LU/LC class (such as buildings, settlements, and water bodies) was assigned a value of zero.

*Rainfall.* Rainfall data for the 18 years were obtained from several agencies. Rainfall data from 35 climatological stations was provided by the National Bureau of Meteorology, Climatology, and Geophysics (BMKG), Citarum Ciliwung River Basin Center (BBWS), and PT Jasa Tirta II with locations spread across Bandung, Bandung Geophysics, Cicalengka, Pamanukan, Cikarang Dam, Cikao Bandung, Jatiasih, Bekasi Dam, and Coral (Figure 3).

The rainfall data analysis results were divided into three time periods, each of which lasted six years. During the first six years, the annual average precipitation in the Citarum RBU varied from 676 to 3,894 mm year$^{-1}$ (2000–2012). Furthermore, the average rainfall at the study site was 817–3,446 mm year$^{-1}$ for the 2012–2018 analysis period and 789–3,284 mm year$^{-1}$ for the 2000–2018 analysis period.

By processing statistics on the average yearly rainfall at each rainfall station, the necessity for a yearly rainfall map in modeling with InVEST was fulfilled. Calculations were carried out for each period. Furthermore, the average rainfall data at each station was analyzed using a spline interpolation technique using the ArcGIS tool.

*Evapotranspiration.* Maximum and minimum air temperatures, extraterrestrial solar energy, and minimum and monthly rainfall were used to calculate daily extraterrestrial radiation from the sun for each rainfall station, create the yearly benchmark evapotranspiration plot, and add the findings to get monthly values. The monthly outer space solar radiation map was created using the spline interpolation technique once more.

Many researchers have applied satellite data to compute air temperature (Sun et al. 2005, Septiangga and Yuniar 2017, Ermida et al. 2020). Landsat 8 has been intensively used to derive land surface temperature, Ermida et al. (2020) calculated LST from Landsat 8 climate data records using the Statistical Mono-Window (SMW) algorithme. The method relied on an empirical relationship between calibrated TOA brightness temperatures in a single TIR channel and LST. In this study, we used the Google Earth Engine (GEE) to collect Landsat 8 Collection 1 Tier 1 calibrated top-of-atmosphere (TOA) reflectance data and employ simple linear regression. For more information on how Radiance and Reflectance are calculated as part of TOA computation see Chander et al. (2009).

A linear regression model was used to validate Landsat 8 LST using imagery from Landsat 8 and ground-based LST. The validation used 60 points LST ground based distributed among the LST in-situ (1 Bandung, 8 Geofisika Bandung, 13 Saguling, 18 Cirata, and 32 Pamanukan) stations. The relationship between air temperature derived from Landsat TM band 10 and LST ground based obtained a linear regression model of landsat
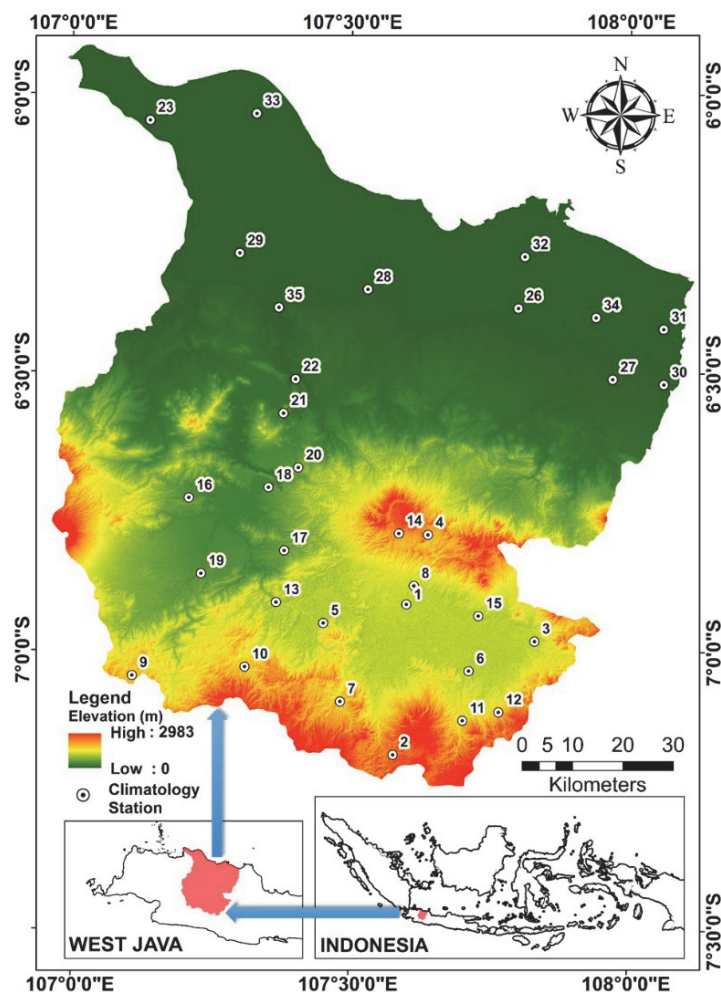


**Fig. 3.** Distribution of climatology observation stations in the Citarum RBU

8 band 10 with the equation result showed y = 0.082x + 15.751, where x is air temperature in Celsius. Validation of the model shows the coefficient of determination ($R^2$) 0.526, and Root Mean Square (RMSE) 0.213. The results show a significant relationship for Landsat 8 to estimate LST in study area.

The lack of data on air temperature gathered from local meteorological stations is an obstacle in preparing air temperature maps. Alternatively, the mean maximum and minimum air temperatures calculated from global climate data (1 km spatial resolution) were resampled to a 30 m spatial resolution (Hijmans et al. 2005). The processing results using a raster calculator show that the annual reference evapotranspiration value varied between 792–1,921 mm year$^{-1}$ (2000), 764–1,749 mm year$^{-1}$ (2012), and 794–2,039 mm year$^{-1}$ (2018).

***Soil Solum Depth and Plant Available Water Content (PAWC).*** The research area had ten soil types, according to BBWS Citarum data: (1) alluvial, (2) andosol, (3) latosol, (4) regosol, (5) grumusol, (6) lithosol, (7) Mediterranean, (8) gley humus, (9) Podsolic, and (10) resin. The soil solum depth was calculated using the map of land system. PAWC was calculated using Saxton, K. S software based on texture and soil type (Saxton 2022). To deal with the soil scarcity properties data, default values were used in the InVEST model for other factors.

***Watershed Boundaries.*** The InVEST model, shapefile format, requires watershed and its 19 sub-watershed boundary data as its inputs. BBWS Citarum-Ciliwung provided information on the Citarum watershed and sub-watershed boundaries.

Water Yield estimation using the InVEST Model were calculated using formula. The yearly water yield for a given LU/LC at each pixel, $Y_{(x)}$, was set in the following manner using equation 1 (Sharp et al. 2015):

$$Y_{(x)} = \left(1 - \frac{AET_{(x)}}{P_{(x)}}\right) \times P_{(x)} \qquad (1)$$

where $AET_{(x)}$ is the yearly evapotranspiration measured at the pixel x and $P_{(x)}$ is the annual precipitation at pixel $x$.

For the vegetated type of LU/LC (Zhang et al. 2004), $\frac{AET_{(x)}}{P_{(x)}}$ i is spatially explicit in its estimation of pixel x, which is calculated using equation 2:

$$\frac{AET_{(x)}}{P_{(x)}} = 1 + \frac{PET_{(x)}}{P_{(x)}} - \left[1 + \left(\frac{PET_{(x)}}{P_{(x)}}\right)^{\omega}\right]^{\frac{1}{\omega}} \qquad (2)$$

where $PET_{(x)}$ denotes pixel x's potential evapotranspiration, and is the non-physical variable that determines the interaction between climate and soil conditions, also known as the coefficient of plant accessible water capacity.

To compute the potential evapotranspiration, PET(x), the formula used was:

$$PET_{(x)} = ET_{0(x)} \times K_{c(x)} \qquad (3)$$

where $ET_{0(x)}$ is the evapotranspiration reference at pixel x and $K_{c(x)}$ is the evapotranspiration coefficient of vegetation at pixel x related to its LU/LC (Fu 1981).

The plant's coefficient of water capacity available at each pixel, $\omega_{(x)}$ referring to Montazar et al. (2020), was calculated in the following manner:

$$\omega_{(x)} = Z \times \frac{AWC_{(x)}}{P_{(x)}} + 1.25 \qquad (4)$$

where $AWC_{(x)}$ is the plant available water capacity volume (mm), and Z is the seasonality factor/Zhang coefficient, an empirical constant that reflects the local rainfall pattern and other hydrogeological factors. In this experiment, the Z value was set to 4, the recommended number for tropical watersheds (Dissanayake et al. 2019). The physical and non-physical elements that define the properties of natural climatic soils are covered in this section.

The quantity of water retained in the soil and released for plant use was determined by $AWC_{(x)}$ (Hamel and Guswa 2015). This variable was derived using PAWC, the depth of the minimum root limiting layer, and the rooting depth of the vegetation in the following manner:

$$AWC_{(x)} = Min(Rest.layer.depth, root.depth) \times PAWC \qquad (5)$$

$ET_{0(x)}$ indicates local climatic conditions based on reference plant evapotranspiration at that site. On the other hand, $K_{c(x)}$ is primarily defined by the vegetation characteristics of each pixel's land use/cover.

Actual evapotranspiration was calculated using reference evapotranspiration data, $ET_{0(x)}$. While non-vegetation has an upper limit dictated by rainfall in this way:

$$AET_{(x)} = Min(K_{c(x)} \times ET_{0(x)}, P_{(x)}) \qquad (6)$$

The modified Hargreaves equation by Gentilucci et al. (2021) was used to determine reference evapotranspiration (mm day$^{-1}$), $ET_{0(x)}$ with the following equation:

$$ET_{0(x)} = 0.0013 \times 0.408 \times Ra \times \left[\left(\frac{T_{max} + T_{min}}{2}\right) + 17\right]$$
$$\times [(T_{max} - T_{min}) - 0.0123P]^{0.76} \qquad (7)$$

where Ra is the extraterrestrial solar radiation (MJ.m$^{-2}$.day$^{-1}$), T_max is the average maximum daily air temperature (°C), T_min is the average minimum daily air temperature (°C), and P is the monthly rainfall (mm day$^{-1}$).

Next, to see the influence and contribution of parameters to fluctuations in water yield volume, we attempted three scenarios in modeling water yield: (1) baseline: no climate or LU/LC change, (2) climate change, but LU/LC in the exact condition, and (3) LU/LC change, but climate in the same condition. By computing the water yield variability under various scenarios, it was possible to quantify the influence of climate as well as LU/LC changes on the variability of water yield using Equations (8) and (9) (Wei et al. 2021):

$$Z_{(C)} = \frac{\Delta\,Climate}{\Delta\,Climate + \Delta\,LULC}\, x\,100\% \qquad (8)$$

$$Z_{(L)} = \frac{\Delta LULC}{\Delta\,Climate + \Delta\,LULC}\, x\,100\% \qquad (9)$$

where $Z_{(C)}$ is climatic rate contribution to alteration in water yield in the absence of LU/LC change, while $Z_{(L)}$ denotes the

rate at which LU/LC contributes to changing water yield in the absence of climate change. Δ *Climate* demonstrates the variation in annual mean water yield from (2000 to 2012) and (2000 to 2018) under a non-LU/LC change scenario, and Δ *LU/LC* indicates the difference between the mean annual water yield from (2000 to 2012), and (2000 to 2018) under a non-climate change scenario.

Dataset from the Geospatial Information Agency validated the water yield model resulting from InVEST (Badan Informasi Geospasial 2015). To validate the model, the coefficient of determination ($R^2$), Pearson correlation (r), and root mean square error (RMSE), were calculated. Linear regression analysis was performed on both the observed data and the model.

*Water Yield Change's Driving Factors*
Multiple linear regression (MLR) analysis was conducted to ascertain a relationship between dependent variables (change of water yield) and land use, climate, socio-economic, and landscape as independent variables. The analysis was carried out using the R studio software. In order to obtain an optimal regression model, the major task at the initial stage was to select the key variables, eliminate unnecessary variables and ensure that the explanatory variables are not multicollinear, based on the Variance Inflation Factor (VIF) value.

A significance test was performed to ensure that the sample used was typically distributed, which compares the sample distribution with the normal distribution to ascertain whether the data show serious deviations from normality. The normality test methods were the Kolmogorov-Smirnov (K-S) and the Shapiro-Wilk tests.

Subsequently, variable ranking was performed to determine the most critical variable based on its contribution rate in the model. We computed the contribution rate by comparing the difference of the residual sum of squares (RSS) value between the MLR results with all variables ($RSS_i$) and without the variable whose contribution was calculated ($RSS_j$). Due to the relative nature of contribution rate values, the aggregation of such values as overall predictors was 100. The formula for calculating the contribution rate (CR) is written as:

$$CR \, (\%)_{(j)} = \frac{RSS_j - RSS_i}{RSS_j} * 100 \qquad (10)$$

Initially, we created a simple model (model A) to examine the consequences of changes in determining forces on the water yield alteration over 18 years (from 2000 to 2018). The model is as follows:

$$Model \, A: \Delta Y = \beta_0 + \beta_1 \Delta X_1 + \beta_2 \Delta X_2 + ... + \beta_i j \Delta X_i + \varepsilon \quad (11)$$

where $\Delta Y$ is the change in the sub-watershed level, $\Delta X_i$ is the change in an explanatory variable between 2000 and 2018, $\beta_i$ is the model coefficient, $\beta_0$ is the intercept, and $\varepsilon$ is the error term.

In the second stage, we modified model A by introducing several combinations of interaction effects between landscape fragmentation metrics and socio-economic factors (social--ecological model). The modified model formula is stated as follows:

$$\Delta Y = \beta_0 + \alpha\beta_{01} \Delta X_1 + \alpha_2 \Delta X_2 + ... + \beta_m \Delta X + \\ + \eta + \alpha_j \Delta X_j \Delta X_0 \qquad (12)$$

where $\Delta X_j \Delta X_0$ denotes the interaction effect between $\Delta X_j$ (the landscape metrics) and $\Delta X_0$ (the socio-economic factors), $\alpha_j$ denotes the model coefficient, $\eta$ denotes the error term. The significance of each interaction model was compared, whether it strengthens or reduces changes in water yield.

***Geographically Weighted Regression (GWR).*** SES is influenced by various interdependent elements, namely biophysical (climate, LU/LC, landscape), socio-economic, and integration socio-economic with the landscape. The GWR techniques can find relationships between dependent and explanatory variables when spatial influence is considered (Fang et al. 2021). Several previous studies have used the GWR method to simulate the spatial distribution model relationship between vegetation and rainfall and to identify the water yield ecosystem service's driving parameter (Zhang et al. 2021).

GWR augments the standard regression by qualifying the estimation of local rather than global parameters. The GWR model is given by Fotheringham et al. (2002):

$$y_i = \beta_{0(u_i,v_i)} + \sum_k \beta_{k(u_i,v_i)} x_{ik} + \varepsilon_i \qquad (13)$$

where $(u_i, v_i)$ denotes the coordinates of the ith point. By considering the location of the dependent variable, the GWR model carries out separate regression at each observation and limits the number of observations used in the regression based on a specific distance to the observed location. Accordingly, the estimates parameters will become local and vary in each location.

This study implements the GW model package in R (Gollini et al. 2015) for data processing. We chose the Gaussian function [exp (–.5 * (vdist/bw)^2)] to compute weights and the Akaike Information Criterion (AIC) approach to find the optimum bandwidth. The bandwidth defines the spatial coverage to limit a subset of points used in the regression. It can be calculated using a fixed kernel (a fixed distance) or adaptive kernel, where the bandwidth corresponds to the number of nearest neighbors.

This study used adaptive and fixed kernels to compute the bandwidth. The models from Ordinary Least Square (OLS), fixed GWR (FGWR), and adaptive GWR (AGWR) were compared, and their quality was assessed in terms of the coefficient of correlation (r) and the residual sum of squares (RSS).

## Results

### Water Yield Spatio-Temporal Dynamic
The analysis of land use /land cover maps obtained area data for each type of LU/LC (Table 3). In Table 3, the dominant types of LU/LC are Paddy Field (45.1%), Plantation Forest (11.91%), Settlement Area (9.54%), Pure Dry Agriculture (8.12%), and Mixed Dry Agriculture (7.47%). The composition of land cover types in 2012 and 2018 is relatively the same as the land cover conditions in 2000 (Table 3).

Changes in land use and spatial land cover (LU/LC) in the Citarum watershed from 2000 to 2018 show Virgin Forest,

Estate Crops Plantation, Plantation Forest Shrub, Shrub, Bare land, and Paddy Filed decreased. There was a decrease in Virgin Forest by 35.87%, Plantation Forest – 13.87%, Shrub – 77.97%, Estate Crops Plantation – 20.24%, Bare land – 24.56% and Paddy Filed – 6.57%.

Meanwhile, other types of LU/LC tend to increase. Settlement area gradually increased to 4.23%, Pure Dry Agriculture to 64.85%, and Mixed Dry Agriculture to 64.85%. This change in LU/LC type will affect the availability of water yields.

According to the InVEST model analysis findings, water yield volume at the Citarum RBU in 2018 was approximately 12.16 billion $m^3$ $year^{-1}$ (Table 4 and Figure 4).

In water yield, the most significant decrease occurred in the Cisadari sub-watershed of 1,241.38 mm (69.00%), and the smallest occurred in the Cibadak sub-watershed of 98.74 mm (13.16%). Meanwhile, the Cibanteng sub-watershed increased by 2.83%. The water yield average depth in 2000 was 1,373.00 mm, while in 2018, it was 764 mm.

Citarum sub-watershed has a maximum yearly rainfall of 1,994 mm $year^{-1}$ with a minimum evapotranspiration potential of 1,291 mm $year^{-1}$. This water yield reflects the natural river flow and does not consider human activities' daily needs, including industry, households, and agriculture (Van Paddenburg et al. 2012). As for 649 mm $year^{-1}$ of actual evapotranspiration, amongst all sub-watersheds in the Citarum RBU, the four sub-watersheds with the highest water yields are the Citarum sub-watershed (1,220 mm $year^{-1}$), Cipunara sub-watershed (1,126 mm $year^{-1}$), Cimalaya sub-watershed (974 mm $year^{-1}$), and Ciasem sub-watershed (969 mm $year^{-1}$), sequentially.

The Citarum sub-watershed is the widest, giving the most significant contribution to water yield, which is 8.05 billion $m^3$ $year^{-1}$ (66.18%), followed by the Cipunara sub-watershed at 1.44 billion $m^3$ $year^{-1}$ (11.89%), the Ciasem sub-watershed at 0.71 billion $m^3$ $year^{-1}$ (5.83%), and the Cimalaya sub-watershed 0.51 billion $m^3$ $year^{-1}$ (4.17%).

The water yield spatial distribution of the Citarum RBU in 2000 is shown in Figure 4a and Figure 4b for 2018. The most

**Table 3.** Area of LU/LC classification of 2000, 2012, and 2018 in Citarum RBU

| No | LU/LC type | 2000 | | 2012 | | 2018* | | 2000–2012 | | 2000–2018 | |
|---|---|---|---|---|---|---|---|---|---|---|---|
| | | Ha | % | Ha | % | Ha | % | Ha | % | Ha | % |
| 1 | Virgin Forest | 43.63 | 3.85 | 29.07 | 2.57 | 27.98 | 2.47 | -14.56 | -33.37 | -15.65 | -35.87 |
| 2 | Plantation Forest | 134.85 | 11.91 | 121.39 | 10.73 | 116.14 | 10.26 | -13.46 | -9.98 | -18.71 | -13.87 |
| 3 | Shrub | 33.55 | 2.96 | 19.61 | 1.73 | 7.39 | 0.65 | -13.94 | -41.55 | -26.16 | -77.97 |
| 4 | Estate Crops Plantation | 63.97 | 5.65 | 56.73 | 5.01 | 51.02 | 4.51 | -7.24 | -11.32 | -12.95 | -20.24 |
| 5 | Settlement Area | 108.04 | 9.54 | 112.61 | 9.95 | 108.8 | 9.61 | 4.57 | 4.23 | 0.76 | 0.70 |
| 6 | Bare land | 10.34 | 0.91 | 9.98 | 0.88 | 7.8 | 0.69 | -0.36 | -3.48 | -2.54 | -24.56 |
| 7 | Lake | 16.42 | 1.45 | 16.39 | 1.45 | 16.4 | 1.45 | -0.03 | -0.18 | -0.02 | -0.12 |
| 8 | Pure Dry Agriculture | 91.94 | 8.12 | 317.55 | 28.06 | 151.56 | 13.39 | 225.61 | 245.39 | 59.62 | 64.85 |
| 9 | Mixed Dry Agriculture | 84.52 | 7.47 | 144.8 | 12.79 | 132.99 | 11.75 | 60.28 | 71.32 | 48.47 | 57.35 |
| 10 | Paddy Filed | 510.56 | 45.10 | 269.37 | 23.8 | 477.02 | 42.15 | -241.19 | -47.24 | -33.54 | -6.57 |
| 11 | Fishpond | 34.08 | 3.01 | 34.07 | 3.01 | 34.47 | 3.05 | -0.01 | -0.03 | 0.39 | 1.14 |
| 12 | Airport | 0.19 | 0.02 | 0.19 | 0.02 | 0.19 | 0.02 | 0.00 | 0.00 | 0.00 | 0.00 |

* Source: Nahib et al. 2021

**Table 4.** Water yield in Citarum RBU from 2000 to 2018

| Catchment Area | Total Water Yield | | | Change in Total Water Yield | | | | | |
|---|---|---|---|---|---|---|---|---|---|
| | billion $m^3$ $year^{-1}$ | | | Percentage (%) | | | Class of change | | |
| | 2000 | 2012 | 2018* | 2000–2012 | 2012–2018 | 2000–2018 | 2000–2012 | 2012–2018 | 2000–2018 |
| Citarum | 9.87 | 8.17 | 8.05 | -17.18 | -1.47 | -18.4 | NC | NC | NC |
| Cipunara | 1.83 | 1.57 | 1.44 | -14.31 | -7.87 | -21.06 | NC | NC | D |
| Ciasem | 1.12 | 0.83 | 0.71 | -26.25 | -14.18 | -36.71 | D | NC | D |
| Cimalaya | 0.99 | 0.61 | 0.51 | -38.10 | -17.21 | -48.76 | D | NC | ED |
| Cikarokrok | 0.31 | 0.32 | 0.24 | 4.92 | -25.77 | -22.11 | NC | D | D |
| Others** | 2.53 | 1.64 | 1.22 | -35.31 | -25.8 | -52.00 | D | D | ED |
| SWS Citarum | 16.64 | 13.14 | 12.16 | -21.07 | -7.38 | -26.91 | D | NC | D |

 * Source: Nahib et al. 2021
** Sum of 14 Catchment areas,
ED = Extremely Decrease (<40%), I = Increase (20–40%), D = Decrease (-20% – -40%),
EI = Extremel Increase (> 40%), NC = Non Change (-20%–20%)

significant change in the concentration of water yield values was found in the sub-watershed Citarum in 2000, and in 2018 it was found in several locations in the Citarum and Cipunara sub-watershed areas. The condition of water yields in 2018 decreased by $4.48 \times$ billion m$^3$ year$^{-1}$ (26.91%) compared to the condition of water yields in 2000. The water yield reduction occurred in all sub-watersheds with varying decreasing levels (2000–2012) and (2012–2018).

According to the Mean Water Yield (MWY) change from 18 years period (Figure 4c), around 45% of the Citarum RBU area, the status Non-Change (NC) spread from the north to the southern part of the Citarum sub-watershed. Meanwhile, 32% of the Citarum RBU area comes under Extremely Decrease (ED).

The results show that the status of Extremely Decrease (ED) is experienced by six sub-watershed areas on the north coast of Java, namely Cisedari, Cisaga, Sewo, Sukamaju, Bugel, and Cidongkol. Otherwise, most of the upstream part of the Citarum sub-watershed area (>50%) is NC status. A Decrease (D) status occurred in 19% of all Citarum RBU areas.

Based on changes in water yields shown in Figure 4c and Table S1, 11 sub-watersheds belong to ED, five sub-watersheds belong to D, and three sub-watershed belong to NC. Most sub-watersheds that underwent ED alterations had an area of fewer than 25,000 hectares, except for the Cibodas (26,251 ha), Cidongkol (29,127 ha), and Cimalaya (52,063 ha). Meanwhile, there are four sub-watersheds with SD status with



(a) Year 2000

(a) Year 2018

(a) Year 2000 – 2018
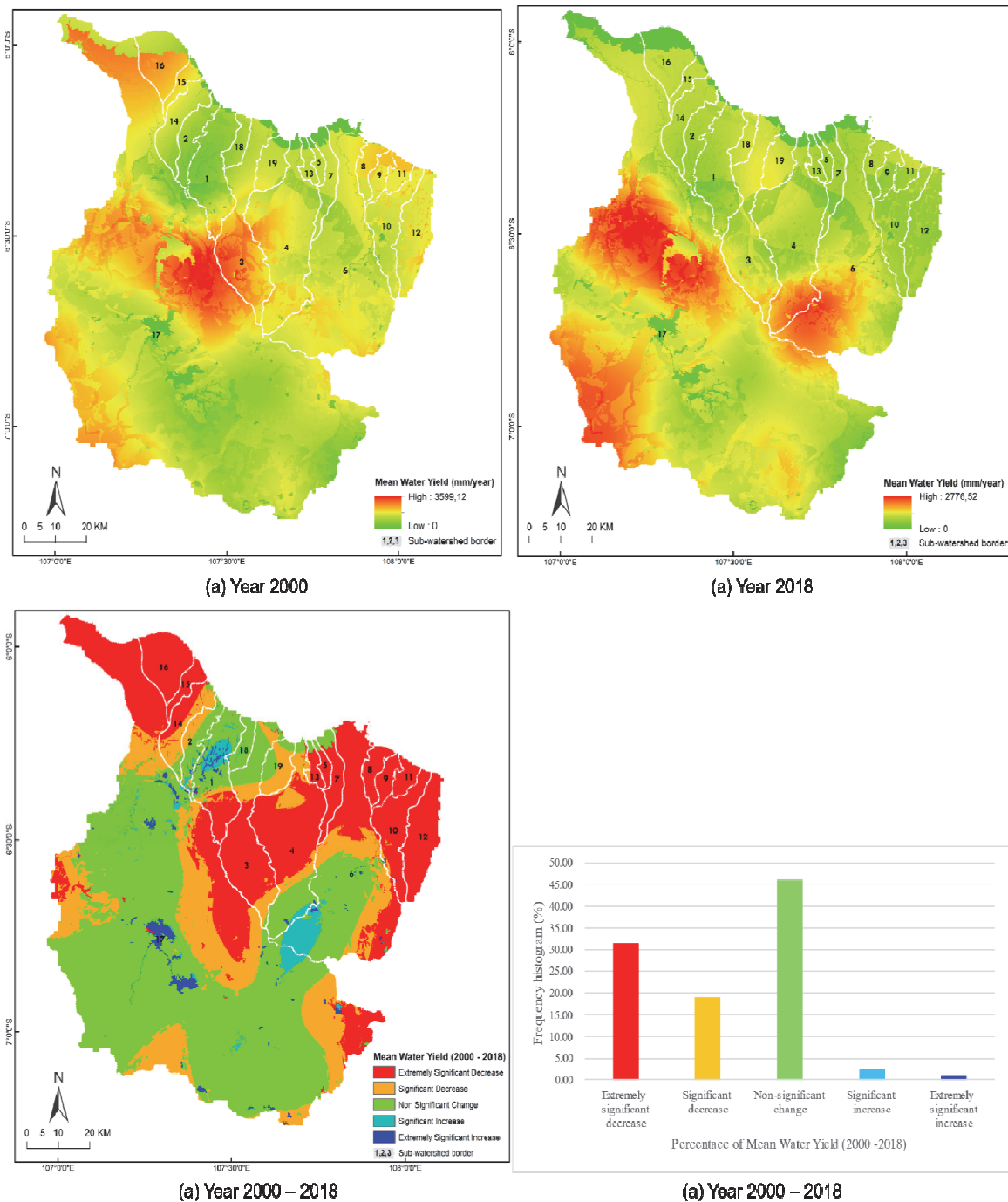
(a) Year 2000 – 2018

**Fig. 4.** Spatial distribution of water yield (a) in the year 2000, (b) in the year 2018, (c) water yield change from 2000–2018, (d) water yield change from 2000–2018 (%) in Citarum RBU

an area of more than 25,000 ha, namely Cipunara (128,059 ha), Ciasem (73,192 ha), and Cikarokrok (36,329 ha). Although there are only three sub-watersheds with NC status, these sub-watersheds have a significant role in terms of area, namely the Citarum sub-watershed with an area of 659,501 ha (58.25%), which can be used as an indicator of changes in water yields in the Citarum RBU.

The InVEST model was validated using validation data for water yield from the Citarum RBU published by Badan Informasi Geospasial (2015) by combining this water yield data with the modeling data. Linear regression analysis between the model (Y) and the observations (X) of water yield deliver a coefficient of determination $(R^2) = 0.9885$, coefficient of Pearson correlation $(r) = 0.994{,}2$ and the mean square error (RMSE) = 0.7 with equation $Y = 0.8682x + 0.2798$.

The actual water yield for the catchment area of all sub-watersheds in the Citarum RBU was calculated, then a model simulation was implemented by including two scenarios without land-use change and climate change parameters. Detailed results of the five sub-watersheds having upstream and downstream sections are shown in Table 5.

The impact of water yield change in 2012 and 2018 without climate change is quite overestimated compared to actual conditions. The models considering climate change scenarios are close to actual conditions, consistent with prior study (Balis et al. 2022), which found that climate significantly influences runoff coefficients.

To prove the results in Table 5, we calculated the contribution level of each parameter included in scenarios, LU/LC and climate change. Equations (8) and (9) explored

the contribution level. Table 6 compared two scenarios to the actual condition and revealed the contribution rate between climate change $(Z_C)$ and LU/LC change $(Z_L)$ to the water yield.

Climate change, particularly rising temperatures and rainfall changes, has a substantial impact on agricultural output through extreme weather – droughts and heat waves. Crop yields are highly dependent on water availability at the plant development stage. Projections of water availability indicate that the cost of obtaining water will continue to increase. Currently, evapotranspiration exceeds rainfall in summer, which causes water storage depletion (at the surface, in the soil, in the soil) (Szwed et al. 2010).

3.2. Water Yield Change's Driving Factors

Based on the spatial pattern, there is a degree of spatial autocorrelation to the water yield at the sub-watershed level. The value of the Moran I coefficient is 0.17 with a score of $Z = 5.50$ (significantly higher than 2.58 and more than 1% in the level of significance test), revealing that changes in spatial distribution at the sub-watershed level are clustered rather than random. This theory is the foundation for the GWR model, which investigates the independent variables' spatial effects on changes in water yields. Diagnostic parameters of the OLS and GWR models are shown in Table 7.

According to Table 7, the larger $R^2$ and smaller AIC values are obtained for the GWR model compared to the OLS model. Based on this, it can be concluded that the GWR model estimation gives better results than the OLS model. The local linear model performed well in the study area, as indicated by $R^2$ values of more than 80%. The high local $R^2$ values ranged from 0.7977 to 0.8359 across the study area (Figure 5).

**Table 5.** Total water yield under different scenarios for 2000–2018 in Citarum RBU

| Catchment Area | | Actual Conditions | | | Conditions without | | | |
|---|---|---|---|---|---|---|---|---|
| | | | | | Climate Change | | Land Use Change | |
| | | billion m³ year⁻¹ | | | billion m³ year⁻¹ | | billion m³ year⁻¹ | |
| Name | 10³ Ha | 2000 | 2012 | 2018 | 2012 | 2018 | 2012 | 2018 |
| Citarum | 659.501 | 9.87 | 8.17 | 8.05 | 9.97 | 9.93 | 8.09 | 7.99 |
| Cipunara | 128.059 | 1.83 | 1.57 | 1.44 | 1.88 | 1.83 | 1.53 | 1.44 |
| Ciasem | 73.192 | 1.12 | 0.83 | 0.71 | 1.19 | 1.12 | 0.77 | 0.71 |
| Cimalaya | 52.063 | 0.99 | 0.61 | 0.51 | 1.05 | 0.99 | 0.57 | 0.51 |
| Cikarokrok | 36.329 | 0.31 | 0.32 | 0.24 | 0.34 | 0.31 | 0.29 | 2.37 |
| Others* | 183.058 | 2.53 | 1.64 | 1.22 | 2.66 | 2.54 | 1.56 | 1.21 |
| Total | 1.132.202 | 16.64 | 13.14 | 12.16 | 17.09 | 16.92 | 12.81 | 12.09 |

* Sum of 14 Catchment Area

**Table 6.** Contribution of Climate (C) and LU/LC (L) to water yield change in Citarum RBU

| Actual 2000 | WT$_{Climate}$ | WT$_{LU/LC}$ | LU/LC(L) | Climate(C) | Total L+C | Z$_L$ (%) | Z$_C$ (%) |
|---|---|---|---|---|---|---|---|
| | 2012 | 2012 | | | | | |
| 16.64 | 17.09 | 12.81 | 0.45 | -3.83 | 4.28 | 10.42 | -89.57 |
| | 2018 | 2018 | | | | | |
| 16.64 | 16.92 | 12.09 | 0.28 | -4.54 | 4.82 | 5.8 | -94.19 |

The contribution level of LU/LC to changes in water yields in the Citarum RBU in the 2000–2018 period ranges from 5.8–10.42%. Meanwhile, the more significant contribution was made by climate change, around 89.57–94.19%.

www.czasopisma.pan.pl  PAN POLSKA AKADEMIA NAUK  www.journals.pan.pl

14  I. Nahib, W. Ambarwulan, D. Sutrisno, M. Darmawan, Y. Suwarno, A. Rahadiati, J. Suryanta, Y. Prihanto, A.W. Rudiastuti, Y.L. Gaol

Based on the analysis of the multicollinearity of the independent variables, we obtained variables that do not have multicollinearity with other variables. Table S2 shows variables that do not significantly change the water yield. The results of multiple regression analysis using R studio software showed nine variables with significant contributions to water yields (Table 8).

In Table 8, variables from climate (mean rainfall) and land use (area of pure dry agriculture, area of bare land, and area of shrubs) were revealed as the primary controlling factors for changes in water yield, with a significant contribution rate of 79.28%. The highest contribution came from the average rainfall factor (28.53%), pure dry agriculture (27.73%), and bare land (15.03%).

Total land use factors give the most significant contribution to water yields, which is 50.75%, more significant than the climate factor. The contribution rate could positively and negatively impact the water yield, where pure dry agriculture and shrub positively impact while the bare land variable is the opposite. On the other hand, the landscape-level factor contributes less than 10% to the water yield. CONTAG and AI have positive impacts; however, LPI and FRAC_MN have negative impacts.

Socio-economic changes in Gross Domestic Product (GDP) per capita indicate a positive relationship to water yields. An increase in GDP per capita will improve infrastructure and increase the built-up area, where a boost in the built-up area results in higher water yield. The GDP per capita variable accounted for 8.58%.

The socio-ecological indicator has both negative and positive effects on water yields depending on the landscape variable and the level of its contribution. The interaction between landscape level and GDP per capita influences water yields with a contribution of 8%, while an increase in GDP per capita changes is integrated with changes in the LPI. The interaction of GDP per capita with the CONTAG variable is positively correlated with changes in water yields. Meanwhile, the interaction of changes in GDP per capita to the FRAC_MN has a negative correlation.

Table 8 indicates the comparison between the simple model (Model A) with the social ecology model (Model B), where the correlation coefficient increase by 0.03 (from 0.76 to 0.79) in Model B. The simple model only considers climate, land use, and landscape variables, while the socio-ecology model added the effect of landscape and socio-economic variables in the water yield estimation. The results of testing on social-ecological variables, i.e., landscape configuration and the effect of social-ecological integration ($\Delta$ LPI * per capita GDP, FRAC * per capita GDP, $\Delta$ AI * $\Delta$ per capita GDP), show that there are changes in the contribution rate of each variable (climate, land-use, landscape, and socio-economic) to water yield. Climate and Socio-economic variables had increased

**Table 7.** Summary OLS Model and GWR Model

| Method | Metrics | | |
|--------|---------|---------|---------|
| | RSS | R² | AIC |
| OLS | 1523.59 | 0.7913 | 161.22 |
| Fixed GWR | 1139.76 | 0.8439 | 143.23 |
| Adaptive GWR | 1140.58 | 0.8438 | 143.25 |
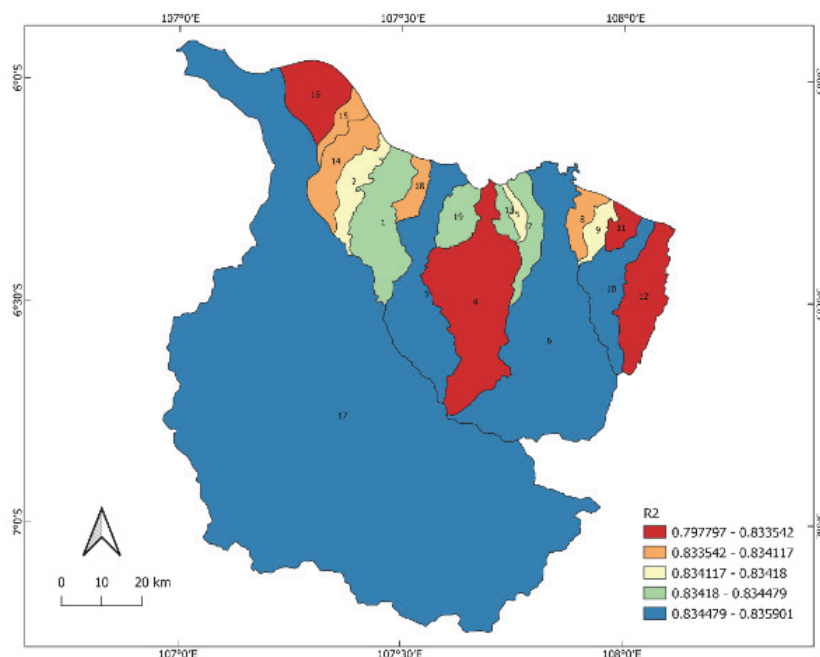


**Fig. 5.** The Local R² of the GWR model

contribution by around 6% and 44%, respectively. Meanwhile, the contribution from the other two variables decreased by –20% (LU/LC) and -40% (Landscape), with a coefficient of determination that is relatively the same as the standard model. In addition, the change in the level of contribution using the social ecology model (increasing climate and land use variables; while decreasing contribution level of landscape) due to the contribution of the landscape variable level is distributed for the landscape and the socio-economic simultaneously. In addition, the social ecology model demonstrates a rising contribution of climate and land use factors but a falling contribution of landscape variables; this is because the contribution of the landscape variable level is simultaneously dispersed for the landscape and the socio-economic variables. Thus, adding socio-ecological variables is better than the standard model.

Based on the same dataset and nine explanatory variables as used in the OLS model, further analysis of the GWR model was carried out. GWR presents 19 local regressions with different predictive coefficient values (Figure S1). Furthermore, the predictive coefficients were classified into three classes, as the five largest sub-watersheds are presented in Table 9.

Based on Figure S1 and Table 9, the prediction coefficient values for each sub-basin are different, indicating the effect of spatial heterogeneity. Their spatial distribution differed from the precipitation and socio-economics distribution, which significantly impacted west water yield more than east.

The local mean regression coefficient for the main controlling factors variables are average rainfall, pure dry agriculture, and bare land, with values of 15.82, 16.93, 13.27, and -8.47, respectively.

## Discussion

### *Water Yield Spatio-Temporal Dynamic*

The Citarum RBU has a water yield of 12.16 billion $m^3$ $year^{-1}$. The MWY is 935 mm $year^{-1}$, consistent with published data

**Table 8.** Results of OLS models (standardized beta coefficients with significant level)

| Model | Model A | | Model B1 | | Model B2 | | Model B3 | |
|---|---|---|---|---|---|---|---|---|
| $R^2$ | 0.7636 | | 0.7848 | | 0.7895 | | 0.7913 | |
| Driving factors | β | CR* (%) | B | CR* (%) | β | CR* (%) | β | CR* (%) |
| **Climate** | | | | | | | | |
| Average precipitation | 15.569 | 28.53 | 15.598 | 30.28 | 17.364 | 30.77 | 16.656 | 30.09 |
| **Land use** | | | | | | | | |
| Shrub | 16.993 | 7.99 | 16.859 | 8.53 | 18.457 | 9.68 | 18.204 | 9.49 |
| Pure Dry Agriculture | 11.806 | 27.73 | 9.977 | 23.77 | 10.068 | 23.56 | 10.068 | 23.38 |
| Bare Land | -6.376 | 15.03 | -2.357 | 10.24 | -2.591 | 10.48 | -1.931 | 9.85 |
| **Landscape** | | | | | | | | |
| LPI** | -0.070 | 2.27 | 0.188 | 1.81 | 0.204 | 1.86 | 0.213 | 2.04 |
| FRAC_MN** | -12.044 | 5.89 | 2.124 | 0.65 | 0.557 | 1.05 | 2.901 | 1.05 |
| CONTAG** | 1.277 | 2.66 | 0.339 | 0.81 | -0.977 | 0.78 | 0.239 | 0.90 |
| AI** | 0.509 | 1.31 | -15.707 | 2.09 | -15.093 | 1.84 | -15.052 | 1.95 |
| **Socio-economic** | | | | | | | | |
| Δ per capita GDP | 5.967 | 8.58 | -8.204 | 13.82 | -7.961 | 12.67 | -8.685 | 13.49 |
| **Effect of Landscape & Socio-economic** | | | | | | | | |
| Δ LPI * Δ per capita GDP | | | 9.072 | 8.00 | | | | |
| Δ FRAC * Δ per capita GDP | | | | | -9.774 | 7.29 | | |
| Δ AI * Δ per capita GDP | | | | | | | 8.736 | 7.74 |

 * CR refers to that contribution rate to change in water yield (%).
** LPI: Largest patch Index, CONTAG: Contagion, FRAC_MN: Mean Fractal Dimension Index, AI: Aggregation Index.

**Table 9.** Predictive coefficients of GWR model

| No | Catchment Area | AP | Sb | PDA | BL | LPI | FM | CG | AI | GDP |
|---|---|---|---|---|---|---|---|---|---|---|
| 1 | Citarum | M | H | L | H | H | H | H | M | H |
| 2 | Cipunara | L | M | L | M | M | H | H | H | H |
| 3 | Ciasem | L | L | L | H | H | H | L | L | H |
| 4 | Cimalaya | H | M | H | L | L | M | H | H | M |
| 5 | Cikarokrok | H | H | H | L | L | L | H | M | L |

L: predictive coefficient low, M: predictive coefficient medium, H: predictive coefficient high, AP: Average Precipitation, Sb: Shrub, PDA: Pure Dry Agricultural, BL: Bare Land, LPI: Largest patch Index, FM: Mean Fractal Dimension Index, CG: Contagion, AI: Aggregation Index, GDP: per capita GDP.

www.czasopisma.pan.pl    PAN    www.journals.pan.pl
POLSKA AKADEMIA NAUK

16   I. Nahib, W. Ambarwulan, D. Sutrisno, M. Darmawan, Y. Suwarno, A. Rahadiati, J. Suryanta, Y. Prihanto, A.W. Rudiastuti, Y.L. Gaol

(BIG 2015, Kementerian Pekerjaan Umum 2016), which shows that the water yield at the Citarum RBU is 12.95 billion $m^3year^{-1}$, and the MWY is 994 mm year$^{-1}$. The water yield's spatial distribution pattern and magnitude from the modeling outcomes are comparable to the result of (Montazar et al. 2020); aside from that, this study's water yield value is significantly lower than the previous outcome.

According to BIG 2015, the Citarum RBU has a large potential water resource of 12.95 billion $m^3$ year$^{-1}$, which is added by heavy rainfall of 2,000–4,000 mm year$^{-1}$ (Kementerian Pekerjaan Umum, 2016). The Citarum RBU yield requires only 7.65 billion $m^3year^{-1}$ of water. The water requirement is made up of the following components: urban water (municipal), 0.03 billion $m^3$ year$^{-1}$ (0.3%), industry, 0.15 billion $m^3$ year$^{-1}$ (2%), maintenance, 0.38 billion $m^3$ year$^{-1}$ (5%), freshwater, 0.49 billion $m^3$ year$^{-1}$ (6%), and irrigation, 6.64 billion year$^{-1}$ (86.7%). The remaining 5.30 billion $m^3year^{-1}$ is made up of potentially wasted water (wasted at sea). Saguling Reservoir (for irrigation/hydropower), Cipanjuang Reservoir (hydropower), Cileunca Reservoir (hydropower), Jatiluhur (irrigation/hydropower), and Cirata Reservoir (hydropower) are the main irrigation facilities and infrastructure that currently supply water needs in the Citarum RBU.

Referring to Patuha's research (Yudistiro et al. 2019), the water yield in Citarum (935.26 – 1,079.27 mm year$^{-1}$) is lower than in the Patuha Mountains area, Bandung Regency, West Java (2,163 mm year$^{-1}$), that shares the same climatic conditions.

These findings are consistent with previous studies (Nahib et al. 2021, Wei et al. 2021), which state that water yield indicates a watershed's health, and a healthy watershed has slight water variation. In 18 years, water yield has decreased by 0–20% (NC), 20–40% (I), and more than 40% (EI). A low level of decreased water yield indicates that the watershed has been well managed, a moderate level of decreased water yield indicates poor watershed management, and a high level of decreased water yield indicates poor watershed management.

The contribution level of LU/LC to changes in water yields in the Citarum RBU in the 2000–2018 period is in the range of 5.8–10.42%. Meanwhile, the more significant contribution was made by climate change, around 89.57–94.19%.

The more dominant climate contribution from changes in LU/LC to changes in water yields in the Citarum is along with research results by Wei et al. (2021), concerning the Shule River Basin, China, which stated that the contribution of climate change to total water yield was higher than LU/LC change. In that case, 90.56% accounted for contribution from climate, and the rest, 9.44%, came from LU/LC change. Moreover, research in the Qinghai River (Lian et al. 2020) also mentioned that LU/LC change contributed 10%, while precipitation dominated water yield (about 90%). A similar result was found in Black Sea Catchment (including Poland) (Rouholahnejad Freund et al. 2017), where the climatic variables were more significant to model the water yield than different land use change scenarios.

The contribution of LU/LC change and climate change is strengthened by research at the exact location, the Citarum upstream. Some research (Nahib et al. 2021; Siswantoto and Frances 2019) confirmed the findings in estimating the relationship of LU/LC to water in the upper side of the Citarum watershed (with the TETIS application, distributed hydrological model). While Nahib et al. (2021) revealed that

climate change has a greater consequences on water yield than changes in LU/LC in the Citarum watershed, the effect of alteration in rainfall (14.06–27.53%) are the most significant, followed by the evapotranspiration effect (10.97–23.86%) and LU/LC (10.29–12.96%). According to Siswantoto and Frances (2019), changing the LU/LC reduces evapotranspiration, which in turn increases water yield by 15% to 40%.

### Water Yield Change's Driving Factors

It is essential to look for drivers' multi-level impact on water yield changes. In order to assess the GWR model, modified $R^2$ was used. The adaptive bandwidth and fixed bandwidth applications do not significantly differ in $R^2$. The application of the GWR model shows that there can be heterogeneity. This condition indicates that the selection of the GWR model is more appropriate than the OLS model. Based on the comparison between the OLS model and the GWR model, the GWR model shows better performance than the OLS model; GWR models have higher $R^2$ and lower AIC and RSS values.

This finding aligns with the results by Wang et al. (2017) which stated that the GWR model is more robust on the driving variable than the OLS method. The GWR model can explain the location-specific and more detailed role of the related factors in influencing changes in water yields, while OLS only produces global coefficients for each explanatory variable.

Precipitation is one of the main variables affecting water yield. The average precipitation at the Citarum RBU decreased from 2,320 mm in 2000 to 1,783 mm in 2018. The InVEST model estimated a corresponding decrease in water yield from 1,469 mm to 1,074 mm.

A positive correlation between rainfall change and water yield change is in line with (Nahib et al. 2021, Sun et al. 2017, Łabędzki and Bąk 2017). Referring to Nahib et al. (2021), the water yield spatial pattern and rainfall in the Citarum RBU have a linear correation, where lower rainfalls are linked with a smaller water yield and vice versa. In general, the mean annual precipitation (MAP) correlates to the MWY linearly, so that a high MAP will lead to a large MWY and vice versa. Anomalies occur in the land use type bare land area, where the amount of rain is relatively high but MWY low. In line with that, the correlation between the variation of water yield and precipitation is positive and the strongest (Sun et al. 2017).

Based on the analysis of the standard rainfall index (SPI) with the crop drought index (CDI), the impact of meteorological climate change (drought) causes crop water deficits and reduces crop yields in various regions of Poland and reduces crop yields. The most obvious impact of drought on cultivated plants is reduced evapotranspiration, resulting in a decrease in crop yields (Łabędzki and Bąk 2017). Meanwhile, Ferencz et al. 2022 reported that an increase in the frequency of torrential rainfall (above 50 mm) favors surface runoff over infiltration As a result, groundwater resources are depleting. Extreme meteorological events, as presented in the study and projected in the future, pose a serious threat to natural groundwater outflow sites.

The correlation between vegetation and water yield depends on the vegetation types; some have a positive correlation, and others the opposite (Nahib et al. 2021, Muhammed et al. 2021). Water yield based on LU/LC in the Citarum RBU depicted shrubs producing the highest average water yield of

1,516 mm year$^{-1}$ (Nahib et al. 2021). The second-largest water yield is from virgin forests (1,444 mm year$^{-1}$), the next is pure dry agriculture (1,348 mm year$^{-1}$), as well as plantation forests (1,226 mm year$^{-1}$).

For long-term studies, the spatial scale of the watershed is critical in determining the hydrological effect of forest cover (Muhammed et al. 2021). On the micro and meso scales, there is no relationship between forest cover and rainfall and water yields. On the other hand, on a global scale, there is a relatively high correlation coefficient (r = 0.77, p 0.05) between forest cover and water yield. According to the findings of the analysis, during the rainy season, deforestation in regional watersheds leads to high discharge and flooding. On the other hand, it exacerbates the dry season flow.

Although the model resolution was coarse about 100 km, to model water yield, researchers combined human impacts, surface interaction, groundwater pumping, and runoff. The study revealed that considering human impacts, such as irrigation and reservoir operation, results in a better water yield model (Pokhrel et al. 2017).

Previous research stated the relationship between landscape level and water yield. Xu et al. (2019) found that from 2000 to 2010, patch richness density (PRD), aggregation index (AI), Shannon's diversity index (SHDI), the construction land (CL) portion, and the average yearly precipitation (AP) were the motivating forces whose explanatory power for the spatial variability of water yields in the Beiyun River Basin, Beijing, was always greater than 30%. AI and AP are the two landscape indices most relevant to annual water yields that are positively correlated with water yield, and the others are the opposite. Besides that, Hu et al. (2020) found that the correlation between landscape heterogeneity and water yields suggests that reduced landscape fragmentation and increased aggregation are beneficial for water conservation. This condition is confirmed by Gwate et al. (2022), where there is an inverse relationship between landscape fragmentation and evapotranspiration (ETo), suggesting that unregulated landscape fragmentation can affect the catchment's water balance.

The water yield in Batu Pahat, Malaysia, using the InVEST model, shows that the vegetated area produces a higher water yield than the built-up area (Ziexin 2020). Meanwhile, Dinka and Chaka discovered that land degradation can jeopardize agricultural sustainability and the availability of natural resources in the area. Similar changes are expected in the future, which could be a major cause of land degradation in the watershed, resulting in decreased crop production and a scarcity of fodder unless proper consideration for natural resource conservation practices is given (Dinka and Chaka 2019).

The landscape metric approach was used to measure land-use landscape patterns at the landscape level, landscape shape index (LSI), specifically patch density (PD), most extensive patch index (LPI), and average patch area (AREA MN). According to the study findings, green open space (GOS) underwent patch loss aggregation and fragmentation. As a result, it is critical to maintaining the vegetation to generate water yield for the area.

Changes in LPI correlated significantly and inversely with changes in water yield. These study results follow Li et al. (2020), where forest fragmentation (vegetated area) was conducive to increasing water yield. Meanwhile, Cao et al. (2009) stated that vegetated area aggregation, on the other hand, reduced water yield by boosting the canopy intercept of precipitation and accelerating water consumption.

Poverty, population growth, and a lack of strong institutional and technological support are the primary drivers of change in LU/LC in watersheds. The majority of changes in watershed areas are the result of reduced agricultural production activities for food self-sufficiency (Dinka and Chaka 2019).

According to Li et al. (2018) research in the Taihu Lake Basin (TLB) of China, the development of local water yields is strongly related to GDP per capita. GDP per capita was found to be positively correlated with water yield. This discovery is consistent with the research results of (Yang et al. 2021, Sun et al. 2017, Li et al. 2018). The increased water yield with GDB per capita and the growth rate of construction land have a firm consistency, with correlation coefficients of 0.89 (p < 0.05) and 0.93 (p < 0.05), respectively.

While the study of Yang et al. (2021) shows that the correlation of GDP per capita to vegetation cover (and the result correlation with water yield) shows no clear pattern, it can be positively or negatively correlated. Research in the Loess Plateau, China, found that the relationship of GDP per capita to vegetation change (individually effect) was positive. In contrast, the comprehensive effect (and other variables) negatively correlated to vegetation change in 2000 and there was a positive correlation in 2015. The variables used in the two periods are the same.

This condition is reinforced by the research findings by Sun et al. (2017), which are affected by natural geographical elements. The spatial distribution of water yield is not following the spatial distribution of social-economic development level, namely GDP and population. In China's Nansi Lake Basin region, a significant positive correlation was found between water yields and socio-economic factors (GDP and population) variations. The increase in GDP will lead to urbanization. The impact of urbanization causes an increase in the development of built-up areas and urban construction lands so that the impermeable water surface increases, encouraging an increase in water yield.

Modeled annual water yield in the 1985–1994 and 2008–2017 periods across catchments in England by Gosal et al. (2017) found that human-driven landscape change, including water abstraction, affected the accuracy of the water yield change model. In more detail, the research result by Redhead et al. (2016) suggests that anthropologically influenced processes have become critical factors in water yield modeling. Since the model is sensitive to variation in the explanatory variables, the selection of input data is critical and should be validated.

The landscape interaction model with GDP per capita shows that the contribution of the individual landscape variables decreases. On the other hand, the GDP per capita variable increases, increasing the contribution of the average rainfall. This finding is in line with the research of Zhang et al. (2021) in the Yangtze River Basin, China, which states that there is no clear correlation between the interaction of per capita income with landscape patterns on water yields. Meanwhile, research conducted by Scown et al. (2017), which explores the socio--ecological conditions of watersheds across the US, shows that

regional averages of the Integrity Watershed Index (IWI) are strongly associated with ecoregions, industrial dependencies, and landscape states in an explicit spatial-regression model ($R^2 = 0.77$, $p < 0.001$). We also identified associations between environmental and socio-economic drivers and watershed integrity, which may prove helpful in developing action plans or large-scale watershed management strategies.

Another research by Bai et al. (2020) combines statistical data and InVEST models in China's TLB region. The study discovered that correlations between characteristic landscape metrics and ecosystem service indicators changed over time for various ecosystem service indicators at the district and pixel scale levels. The impact of characteristic landscape metrics on several ecosystem service indicators, as well as the trade-offs between these ecosystem service indicators, reveals the impact of scale effects on correlations and trade-offs. As a result, planners and managers must consider effective metrics of landscape characteristics and scale effects to improve ecosystem services while minimizing undesirable trade-offs.

Based on the urban and SES approach, the analysis found that the institutional design characteristics of land use regulations (local autonomy regimes), resource productivity, and predictability of land use dynamics – influenced landscape change more intensively during the study period (Deslatte et al. 2022). In the Social ecological model, the correlation coefficient increased by 0.03 (from 0.76 to 0.79), showing a stronger relationship. Besides that, there is an increase in the contribution rate for climate and land-use variables. This condition reveals that the socio-ecological model is superior to the simple model.

## Conclusions

The InVEST model is used to analyze the Spatio-temporal pattern of water yield in the Citarum watershed and local scale watersheds in tropical Indonesia. Meanwhile, to determine the driving factors for changes in water yields, 20 variables were used, consisting of 3 climate variables, nine land use variables, five landscape configuration variables, and three socio-economic variables. The GWR model analyzes the heterogeneity of the factors driving changes in water yields.

In general, the annual water yield decreased from 16.64 billion $m^3$ $year^{-1}$ in 2000 to 12.16 billion $m^3$ $year^{-1}$ in 2018. The decrease in water yield was 4.48 billion $m^3$ $year^{-1}$ ( 26.91%) and almost occurred in all parts of the watershed. However, it was discovered that socio-ecological variables in water yields in the Citarum RBU, such as landscape configuration and the effect of social-ecological integration (LPI * per capita GDP, FRAC * per capita GDP, AI * per capita GDP), show that each variable (climate, land-use, landscape configuration, and socio-economic) contributes differently to water yield. Climate and Socio-economic characteristics contributed 6% and 44%, respectively. LU/LC and Landscape Configuration contributions fell by 20% and 40%, respectively, with a similar coefficient of determination to the conventional model. Adding socio-ecological variables improves the model. The GWR model can explain the site-specific and more detailed role of related factors in influencing changes in water yields, while OLS only produces global coefficients for each explanatory variable.

The biophysical technique for calculating water yields is projected to develop socio-ecological models soon. Adding social variables (such as water costs and community perceptions of natural resources) and testing the model's applicability on various watershed dimensions and features (urban/developed vs rural/underdeveloped areas) are essential to constructing a socio-ecological model. The research methods established here can be utilized in other tropical countries like Indonesia. Finally, this research (social-ecological system) can be applied by planners to monitor and evaluate water resources' availability in sustainably managing watersheds.

### Limitations of this study
Not all meteorology stations record air temperature conditions, so the air temperature we used does not reflect the actual temperature conditions at the meteorological station. The air temperature data used is the estimated temperature of the global air temperature.

### Supplementary Materials
See supplementary material for the complete information regarding the results and datasets for the statistical computation. Table S1 depicts detailed water yield changes in each river basin. Table S2 provides the tolerance and variance inflation factor for each variable included in the training. Table S3 shows data for OLS and GWR training. Figure S1 describes the local spatial distribution of regression coefficients of GWR model.

## References

Ambarwulan, W., Nahib, I., Widiatmaka, W., Suryanta, J., Munajati, S.L., Suwarno, Y., Turmudi T, Darmawan M. & Sutrisno, D. (2021). Using Geographic Information Systems and the Analytical Hierarchy Process for Delineating Erosion-Induced Land Degradation in the Middle Citarum Sub-Watershed, Indonesia. *Frontiers in Environmental Science*, *9*, 710570. DOI:10.3389/fenvs.2021.71057

Badan Informasi Geospasial. (2015). *Pemetaan Dinamika Sumberdaya Alam Terpadu Wilayah Sungai Citarum; [Mapping of the Dynamics of Integrated Natural Resources of the Citarum River Basin];* Cibinong.

Bai, Y., Chen, Y., Alatalo, J.M., Yang, Z. & Jiang, B. (2020). Scale Effects on the Relationships between Land Characteristics and Ecosystem Services – a Case Study in Taihu Lake Basin, China. *Sci. Total Environ.*, 716, DOI:10.1016/j.scitotenv.2020.137083

Balai Besar Wilayah Sungai Citarum-Ciliwung (BBWS Citarum Ciliwung). *Profil BBWS Citarum [Profile of BBWS Citarum].* (http://sda.pu.go.id/balai/bbwscitarum/profil-bbws-citarum/) (09.03. 2022)

Barbieri, M., Barberio, M.D., Banzato, F., Billi, A., Boschetti, T., Franchini, S. & Petitta, M. (2021). Climate change and its effect on groundwater quality. *Environmental Geochemistry and Health*, 1–12. DOI:10.1007/s10653-021-01140-5

Bin, L., Xu, K., Xu, X., Lian, J. & Ma, C. (2018). Development of a Landscape Indicator to Evaluate the Effect of Landscape Pattern on Surface Runoff in the Haihe River Basin. *J. Hydrol*, 566, pp. 546–557. DOI:10.1016/j.jhydrol.2018.09.045

Borowski, P.F. (2020). Nexus between water, energy, food and climate change as challenges facing the modern global, European and Polish economy. *AIMS Geosci*, 6, pp. 397–421. DOI:10.3934/geosci.2020022

Bucała-Hrabia, A. (2018). Land use changes and their catchment-scale environmenta limpact in the Polish Western Carpathians during transition from centrally planned to free-market economics. *Geographia Polonica*, *91*(2), pp. 171–196. DOI:10.24425/aep.2022.140767

Cao, S., Chen, L. & Yu, X. (2009). Impact of China's Grain for Green Project on the landscape of vulnerable arid and semi-arid agricultural regions: A case study in northern Shaanxi Province. *Journal of Applied Ecology*, 46(3), pp. 536–543.

Chander, G., Markham, B.L. & Helder, D.L. (2009). Summary of current radiometric calibration coefficients for Landsat MSS, TM, ETM+, and EO-1 ALI sensors. *Remote sensing of environment*, *113*(5), pp. 893–903.

Deslatte, A., Szmigiel-Rawska, K., Tavares, A.F., Ślawska, J., Karsznia, I. & Łukomska, J. (2022). Land use institutions and social-ecological systems: A spatial analysis of local landscape changes in Poland. *Land Use Policy*, 114, 105937. DOI:10.1016/j.landusepol.2021.105937

Dinka, M.O. & Chaka, D.D. (2019). Analysis of land use/land cover change in Adei watershed, Central Highlands of Ethiopia. *Journal of water and land development*. DOI:10.2478/jwld-2019-0038

Dissanayake, D., Morimoto, T. & Ranagalage, M. (2019). Accessing the Soil Erosion Rate Based on RUSLE Model for Sustainable Land Use Management: A Case Study of the Kotmale Watershed, Sri Lanka. *Springer International Publishing*; Vol. 5, pp. 291–306. DOI:10.1007/s40808-018-0534-x

Ermida, S.L., Soares, P., Mantas, V., Göttsche, F.-M. & Trigo, I.F. (2020). Google Earth Engine Open-Source Code for Land Surface Temperature Estimation from the Landsat Series. *Remote Sens.* 12, 1471. DOI:10.3390/rs12091471

Fang, W., Huang, H., Yang, B. & Hu, Q. (2021). Factors on spatial heterogeneity of the grain production capacity in the major grain sales area in southeast China: Evidence from 530 Counties in Guangdong Province. *Land*, 10(2), 206. DOI:10.3390/land10020206

Ferencz, B., Dawidek, J., & Bronowicka-Mielniczuk, U. (2022). Alteration of yield and springs number as an indicator of climate changes. Case study of Eastern Poland. *Ecological Indicators*, *138*, 108798.

Figueroa, A.J. & Smilovic, M. (2020). Groundwater irrigation and implication in the Nile river basin. *In Global Groundwater* (pp. 81–95). Elsevier. DOI:10.1016/B978-0-12-818172-0.00007-4

Fotheringham, A.S., Brunsdon, C. & Charlton, M. (2002). *Geographically Weighted Regression: The Analysis of Spatially Varying Relationships*; ISBN 978-0-470-85525-6.

Francis, R. & Bekera, B. (2014). A metric and frameworks for resilience analysis of engineered and infrastructure systems. *Reliability engineering & system safety*, 121, pp. 90–103.

Fu, B.P. (1981). On the Calculation of the Evaporation from Land Surface. *Sci. Atmos. Sin*.

Gentilucci, M., Bufalini, M., Materazzi, M., Barbieri, M., Aringoli, D., Farabollini, P. & Pambianchi, G. (2021). Calculation of Potential Evapotranspiration and Calibration of the Hargreaves Equation Using Geostatistical Methods over the Last 10 Years in Central Italy. *Geosci*, 11, DOI:10.3390/geosciences11080348

Glaser, M., Krause, G., Ratter, B. & Welp, M. (2008) Human-Nature--Interaction in the Anthropocene. Potential of Social-Ecological Systems Analysis. [Website], Available from: file:///C:/Users/USER/Downloads/10.4324_9780203123195_previewpdf.pdf (28.07.2022) DOI:10.1111/j.1365-2664.2008.01605.x

Gollini, I., Lu, B., Charlton, M., Brunsdon, C., Harris, P., Gollini, I., Lu, B., Charlton, M., Brunsdon, C. & Harris, P. (2015). GWmodel: An R Package for Exploring Spatial Heterogeneity. *J. Stat. Softw*, 63, pp. 1–50, DOI:10.1080/10095020.2014.917453

Gosal, A.S., Evans, P.M., Bullock, J.M., Redhead, J., Charlton, M.B., Cord, A.F. Johnson, A. & Ziv, G. (2022). Understanding the accuracy of modelled changes in freshwater provision over time. *Science of the Total Environment*, 833, 155042. DOI:10.1016/j.scitotenv.2022.155042

Gwate, O., Dube, H., Sibanda, M., Dube, T., Chisadza, B. & Nyikadzino, B. (2022). Understanding the influence of land cover change and landscape pattern change on evapotranspiration variations in Gwayi catchment of Zimbabwe. *Geocarto International*, 1–17. DOI:10.1080/10106049.2022.2032386

Hamel, P. & Guswa, A.J. (2015). Uncertainty Analysis of a Spatially Explicit Annual Water-Balance Model: Case Study of the Cape Fear Basin, North Carolina. *Hydrol. Earth Syst. Sci*, 19, pp. 839–853. DOI:10.5194/hess-19-839-2015

Horton, R.E. (1933). The role of infiltration in the hydrologic cycle. *Eos. Transactions American Geophysical Union*, 14(1), pp. 446–460.

Hasan, M. (2011). A policy model for sustainable water resources management of Citarum River Basin. Disertasi. Sekolahg pasca Sarjana IPb. http://repository.ipb.ac.id/handle/123456789/53626

Hu, W., Li, G., Gao, Z., Jia, G., Wang, Z. & Li, Y. (2020). Assessment of the impact of the Poplar Ecological Retreat Project on water conservation in the Dongting Lake wetland region using the InVEST model. *Science of the Total Environment*, *733*, 139423. DOI:10.1016/j.scitotenv.2020.139423

Kementerian Pekerjaan Umum. *Rencana pengelolaan sumber daya air Wilayah Sungai Citarum Tahun 2016 [Management Plan of Citarum River Basin]*. Available online: https://www.coursehero.com/file/60545948/Rencana-Pengelolaan-Sumber-Daya-Air-WS-Citarumpdf/ (12.03.2022).

Kubiak-Wójcicka, K. & Machula, S. (2020). Influence of climate changes on the state of water resources in Poland and their usage. *Geosciences*, 10(8), 312. DOI:10.3390/geosciences10080312

Łabędzki, L. & Bąk, B. (2017). Impact of meteorological drought on crop water deficit and crop yield reduction in Polish agriculture. *Journal of Water and Land Development*, *34*(1), 181. DOI:10.1515/jwld-2017-0052

Li, P., Li, H., Yang, G., Zhang, Q. & Diao, Y. (2018). Assessing the hydrologic impacts of land use change in the Taihu Lake Basin of China from 1985 to 2010. *Water*, 10(11), 1512. DOI:10.3390/w10111512

Li, Y., Sun, Y., Li, J. & Gao, C. (2020). Socioeconomic drivers of urban heat island effect: Empirical evidence from major Chinese cities. *Sustainable Cities and Society*, 63, 102425. DOI:10.1016/j.scs.2020.102425

Lian, X.H., Qi, Y., Wang, H.W., Zhang, J.L. & Yang, R. (2019). Assessing changes of water yield in Qinghai Lake Watershed of China. *Water*, 12(1), 11. DOI:10.3390/w12010011

Montazar, A., Krueger, R., Corwin, D., Pourreza, A., Little, C., Rios, S. & Snyder, R.L. (2020). Determination of Actual Evapotranspiration and Crop Coefficients of California Date Palms Using the Residual of Energy Balance Approach. *Water (Switzerland)*, 12, DOI:10.3390/w12082253

Muhammed, H.H., Mustafa, A.M. & Kolerski, T. (2021). Hydrological responses to large-scale changes in land cover of river watershed. *Journal of Water and Land Development*, (50). DOI:10.24425/jwld.2021.138166

www.czasopisma.pan.pl    PAN    www.journals.pan.pl
POLSKA AKADEMIA NAUK

20    I. Nahib, W. Ambarwulan, D. Sutrisno, M. Darmawan, Y. Suwarno, A. Rahadiati, J. Suryanta, Y. Prihanto, A.W. Rudiastuti, Y.L. Gaol

Nahib, I., Ambarwulan, W., Rahadiati, A., Munajati, S.L., Prihanto, Y., Suryanta, J., Turmudi, T. Nuswantoro, A.C (2021). Assessment of the Impacts of Climate and LULC Changes on the Water Yield in the Citarum River Basin, West Java Province, Indonesia. *Sustain*. 13, DOI:10.3390/su13073919

Nahib, I., Amhar, F., Wahyudin, Y., Ambarwulan, W., Suwarno, Y., Suwedi, N., Turmudi T, Cahyana. D., Nugroho, N.P.,Ramadhani, F., Siagian, D.R., Suryanta, J., Rudiastuti. A.W., Lumban-Gaol, Y., Karolinoerita, V., Rifaie, F. & Munawaroh, M. (2023). Spatial--Temporal Changes in Water Supply and Demand in the Citarum Watershed, West Java, Indonesia Using a Geospatial Approach. *Sustainability*, 15(1), 562. DOI:10.3390/su15010562

Nie, Y., Avraamidou, S., Xiao, X., Pistikopoulos, E.N., Li, J., Zeng, Y., Song, F., Yu, J. & Zhu, M. (2019). A Food-Energy-Water Nexus approach for land use optimization. *Science of The Total Environment*, 659, pp. 7–19. DOI:10.1016/j.scitotenv.2018.12.242

Pei, H., Liu, M., Shen, Y., Xu, K., Zhang, H., Li, Y. & Luo, J. (2022). Quantifying impacts of climate dynamics and land-use changes on water yield service in the agro-pastoral ecotone of northern China. *Science of The Total Environment*, 809, p.151–153. DOI:10.1016/j.scitotenv.2021.151153

Pokhrel, X.N., Koirala, S., Yeh, P.J.F., Hanasaki, N., Longuevergne, L., Kanae, S. & Oki, T. (2015). Incorporation of groundwater pumping in a global L and Surface Model with the representation of human impacts. *Water Resources Research*, 51(1), pp. 78–96. DOI:10.1002/2014WR015602

Redhead, J.W., Stratford, C., Sharps, K., Jones, L., Ziv, G., Clarke, D., Oliver, T.H. & Bullock, J.M. (2016). Empirical validation of the InVEST water yield ecosystem service model at a national scale. *Science of the Total Environment*, 569, pp. 1418–1426. DOI:10.1016/j.scitotenv.2016.06.227

Rouholahnejad Freund, E., Abbaspour, K.C. & Lehmann, A. (2017). Water resources of the Black Sea catchment under future climate and landuse change projections. *Water*, 9(8), 598.

Sawicka, B., Barbaś, P., Pszczółkowski, P., Skiba, D., Yeganehpoor, F. & Krochmal-Marczak, B. (2022). Climate Changes in Southeastern Poland and Food Security. *Climate*, 10(4), 57. DOI:10.3390/cli10040057

Saxton, K.E. (2009) Soil Water Characteristics: Hydraulic Properties Calculator. Available online: https://hrsl.ba.ars.usda.gov/soilwater/Index.htm (13.02.2022)

Scown, M.W., Flotemersch, J.E., Spanbauer, T.L., Eason, T., Garmestani, A. & Chaffin, B.C. (2017). People and water: Exploring the social-ecological condition of watersheds of the United States. Elementa: *Science of the Anthropocene*, 5. DOI:10.1525/elementa.189

Septiangga, B. & Juniar, R. 2016. Aplikasi citra Landsat 8 untuk penentuan persebaran titik panas sebagai indikasi peningkatan temperatur Kota Yogyakarta. Conference paper on National Meteorologi and Climatologi, Jakarta, Indonesia, March 2016

Sharp, R., Tallis, H.T., Ricketts, T., Guerry, A.D., Wood, S.A., Chaplin--Kramer, R. & Bierbower, W. (2015). INVEST 3.1.3 User's Guide; California US, https://invest-userguide.readthedocs.io/en/3.5.0/ (12.08.2021)

Sholeh, M., Pranoto, P., Budiastuti, S. & Sutarno, S. (2018). Analysis of Citarum River Pollution Indicator Using Chemical, Physical, and Bacteriological Methods; Vol. 2049;. In AIP Conference Proceedings (Vol. 2049, No. 1, p. 020068). *AIP Publishing LLC*. DOI:10.1063/1.5082473

Siswanto, S.Y. & Francés, F. (2019). How Land Use/Land Cover Changes Can Affect Water, Flooding and Sedimentation in a Tropical Watershed: A Case Study Using Distributed Modeling in the Upper Citarum Watershed, Indonesia. *Environ. Earth Sci.* 78, pp. 1–15. DOI:10.1007/s12665-019-8561-0

Sriyanti, M.G. Indonesia Climate Change Sectoral Roadmap-ICCSR (Synthesis Report). FAO. 2009. 9789793764498. Jakarta: Badan Perencanaan Pembangunan Nasional, 2010

Sun, Y.-J. Wang, J.-F., Zhang, R.-H., Gillies, R.R., Xue, Y. & Bo. Y.-C. (2015). Air temperature retrieval from remote sensing data based on thermodynamics. *Theoretical and Applied Climatology*. 80, pp. 37–48. DOI:10.1007/s00704-004-0079-y

Sun, X.Y., Guo, H.W., Lian, L., Liu, F. & Li, B. (2017). The Spatial Pattern of Water Yield and Its Driving Factors in Nansi Lake Basin. *J. Nat. Resour*, 32, pp. 669–679. DOI:10.11849/zrzyxb.20160460

Suroso, D., Setiawan, B. & Abdurahman, O. (2010). Impact of Climate Change on the Sustainability of Water Supply in Indonesia and The 714 Proposed Adaptation Activities. *Int. Symp. Exhib. Short Course Geotech. Geosynth. Eng. Challenges Oppor. Clim*. Chang. 2010

Szarek-Gwiazda, E. & Gwiazda, R. (2022). Impact of flow and damming on water quality of the mountain Raba River (southern Poland) – long-term studies. *Archives of Environmental Protection*, 48(1), pp. 31–40. DOI:10.24425/aep.2022.140543

Szwagrzyk, M., Kaim, D., Price, B., Wypych, A., Grabska, E. & Kozak, J. (2018). Impact of forecasted land use changes on flood risk in the Polish Carpathians. *Natural Hazards*, 94(1), pp. 227–240. DOI:10.1007/s11069-018-3384-y

Szwed, M., Karg, G., Pińskwar, I., Radziejewski, M., Graczyk, D., Kędziora, A. & Kundzewicz, Z.W. (2010). Climate change and its effect on agriculture, water resources and human health sectors in Poland. *Natural Hazards and Earth System Sciences*, 10(8), pp. 1725–1737. DOI:10.5194/nhess-10-1725-2010, 2010.

Van Paddenburg, A., Bassi, A., Buter, E., Cosslett, C. & Dean, A.A. (2012). *Heart of Borneo: Investing in Nature for a Green Economy*: A Synthesis Report;

Wang, C., Du, S., Wen, J., Zhang, M., Gu, H., Shi, Y. & Xu, H. (2017). Analyzing Explanatory Factors of Urban Pluvial Floods in Shanghai Using Geographically Weighted Regression. *Stoch. Environ. Res. Risk Assess*, 31, DOI:10.1007/s00477-016-1242-6 Water 2020, 12, 11.

Wei, P., Chen, S., Wu, M., Deng, Y., Xu, H., Jia, Y. & Liu, F. (2021). Using the Invest Model to Assess the Impacts of Climate and Land Use Changes on Water Yield in the Upstream Regions of the Shule River Basin. *Water (Switzerland)*, 13. DOI:10.3390/w13091250

Worldmeter. Indonesia Water https://www.worldometers.info/water/indonesia-water/#water-use (26.05.2022)

WWAP (World Water Assessment Programme). 2021. World Water Development Report Volume 4: Managing Water under Uncertainty and Risk; 2012; Vol. 1.

Xu, J., Liu, S., Zhao, S., Wu, X., Hou, X., An, Y. & Shen, Z. (2019). Spatiotemporal dynamics of water yield service and its response to urbanisation in the Beiyun river Basin, Beijing. *Sustainability*, 11(16), 4361.

Yang, C., Fu, M., Feng, D., Sun, Y. & Zhai, G. (2021). Spatiotemporal Changes in Vegetation Cover and Its Influencing Factors in the Loess Plateau of China Based on the Geographically Weighted Regression Model. *Forests*, 12. DOI:10.3390/f12060673

Yang, X., Chen, R., Meadows, M.E., Ji, G. & Xu, J. (2020). Modelling Water Yield with the InVEST Model in a Data Scarce Region of Northwest China. Water Sci. Technol. *Water Supply*, 20, pp. 1035–1045, DOI:10.2166/ws.2020.026

Young, M. & Esau, C. (Eds.). (2015). Investing in water for a green economy: Services, infrastructure, policies and management. Routledge.

Yudistiro, Kusratmoko, E. & Semedi, J.M. (2019). Water Availability in Patuha Mountain Region Using InVEST Model "Hydropower Water Yield." *In Proceedings of the E3S Web of Conferences*; Vol. 125. DOI:10.1051/e3sconf/2019125010

Zhang, L., Hickel, K., Dawes, W.R., Chiew, F.H.S., Western, A.W. & Briggs, P.R. (2004). A Rational Function Approach for Estimating Mean Annual Evapotranspiration. *Water Resour*. Res, 40, pp. 1–14, DOI:10.1029/2003WR002710

Zhang, X., Zhang, G., Long, X., Zhang, Q., Liu, D., Wu, H. & Li, S. (2021). Identifying the Drivers of Water Yield Ecosystem Service: A Case Study in the Yangtze River Basin, China. *Ecol. Indic*, 132. DOI:10.1016/j.ecolind.2021.108304

Zemełka, G., Kryłów, M. & Szalińska van Overdijk, E. (2019). The potential impact of land use changes on heavy metal contamination in the drinking water reservoir catchment (Dobczyce Reservoir, south Poland). *Archives of Environmental Protection*, 45(2), pp. 3–11. DOI:10.24425/aep.2019.127975 ;

Ziexin, H. (2020). *Impact of spatial land use change on green space and water yield in Batu Pahat, Johor* (Doctoral dissertation, Universiti Malaysia Kelantan).

## Supplementary Materials

### Appendix B

**Tabel S1.** Changes in Water Yield at Citarum RBU in 2000 and 2018

| ID | Watershed Name | 2000 mm | 2018 mm | Changes 2000–2018 (mm) | Changes 2000–2018 (%) | Status |
|---|---|---|---|---|---|---|
| 1 | Cikarokrok | 842.65 | 656.34 | -186.31 | -22.11 | D |
| 2 | Cibadak | 750.31 | 651.57 | -98.74 | -13.16 | NC |
| 3 | Cimalaya | 1,901.34 | 974.30 | -927.04 | -48.76 | ED |
| 4 | Ciasem | 1,531.45 | 969.28 | -562.17 | -36.71 | D |
| 5 | Cireungit | 1,072.90 | 534.83 | -538.07 | -50.15 | ED |
| 6 | Cipunara | 1,427.59 | 1,126.94 | -300.65 | -21.06 | D |
| 7 | Cirandu | 1,007.31 | 473.78 | -533.54 | -52.97 | ED |
| 8 | Sewo | 1,725.18 | 700.08 | -1,025.10 | -59.42 | ED |
| 9 | Sukamaju | 1,731.13 | 663.62 | -1,067.51 | -61.67 | ED |
| 10 | Cibodas | 1,411.56 | 616.43 | -795.13 | -56.33 | ED |
| 11 | Bugel | 1,763.13 | 723.96 | -1,039.16 | -58.94 | ED |
| 12 | Cidongkol | 1,571.77 | 590.83 | -980.94 | -62.41 | ED |
| 13 | Batang Leutik | 1,055.72 | 592.31 | -463.41 | -43.90 | ED |
| 14 | Cibadar Dua | 1,208.09 | 756.29 | -451.80 | -37.40 | SD |
| 15 | Cisaga | 1,617.09 | 773.87 | -843.22 | -52.14 | ED |
| 16 | Cisedari | 1,799.12 | 557.74 | -1,241.38 | -69.00 | ED |
| 17 | Citarum | 1,495.98 | 1,220.71 | -275.27 | -18.40 | NC |
| 18 | Cibanteng | 946.56 | 973.33 | 26.76 | 2.83 | NC |
| 19 | Cigemari | 1,237.30 | 953.30 | -284.00 | -22.95 | D |

**Table S2.** Tolerance and Variance Inflation Factor (VIF)

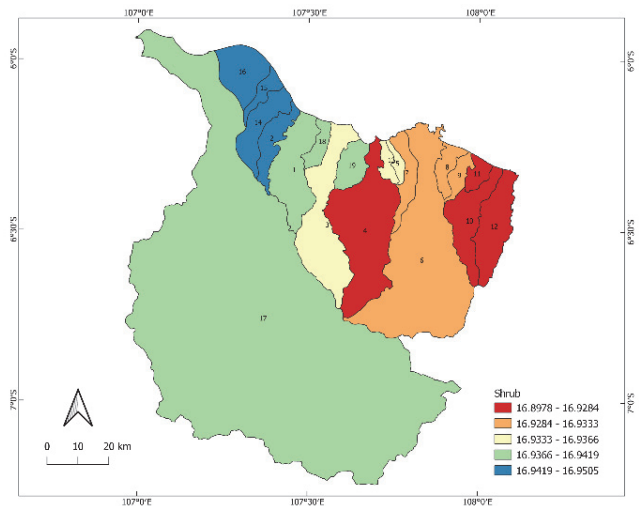| Variables | Tolerance | VIF |
|---|---|---|
| Average precipitation | 0.6991885 | 1.430229 |
| Shrub | 0.1689563 | 5.918689 |
| Pure Dry Agriculture | 0.4497479 | 2.223468 |
| Bare Land | 0.3374543 | 2.963364 |
| Large patch Index | 0.1492413 | 6.700558 |
| Mean Fractal Dimension Index | 0.4337878 | 2.305275 |
| Contagion | 0.3310035 | 3.021116 |
| Aggregation Index | 0.2782403 | 3.594015 |
| Δ per capita GDP | 0.3229058 | 3.096878 |

**Table S3.** Dataset for OLS and GWR training

| ID | Watershed Name | Water Yield Change | Average precipitation | Shrub | Pure Dry Agriculture | Bare Land | Largest Patch Index | Mean Fractal Dimension Index | Contagion | Aggregation Index | Δ per capita GDP |
|---|---|---|---|---|---|---|---|---|---|---|---|
| 1 | Cikarokrok | -22.11 | 2.00 | 1.00 | 2.00 | 1.00 | -0.21 | -0.08 | -0.93 | -0.75 | 3.00 |
| 2 | Cibadak | -13.16 | 3.00 | 1.00 | 2.00 | 1.00 | -10.04 | -0.43 | -7.30 | -0.82 | 3.00 |
| 3 | Cimalaya | -48.76 | 2.00 | 1.00 | 1.00 | 1.00 | -0.57 | 0.17 | -1.39 | -0.15 | 3.00 |
| 4 | Ciasem | -36.71 | 2.00 | 1.00 | 2.00 | 1.00 | 0.00 | 0.00 | 0.00 | 0.00 | 3.00 |
| 5 | Cireungit | -50.15 | 1.00 | 1.00 | 2.00 | 2.00 | 0.00 | 0.00 | 0.00 | 0.00 | 1.00 |
| 6 | Cipunara | -21.06 | 2.00 | 1.00 | 2.00 | 2.00 | 0.00 | 0.00 | 0.00 | 0.00 | 2.00 |
| 7 | Cirandu | -52.97 | 2.00 | 1.00 | 2.00 | 2.00 | -0.77 | 0.38 | -0.77 | -0.06 | 1.00 |
| 8 | Sewo | -59.42 | 1.00 | 2.00 | 1.00 | 2.00 | 0.00 | 0.00 | 0.00 | 0.00 | 1.00 |
| 9 | Sukamaju | -61.67 | 2.00 | 1.00 | 1.00 | 2.00 | 0.00 | 0.00 | 0.00 | 0.00 | 1.00 |
| 10 | Cibodas | -56.33 | 1.00 | 1.00 | 2.00 | 2.00 | 1.71 | 0.07 | 0.70 | 0.02 | 1.00 |
| 11 | Bugel | -58.94 | 2.00 | 1.00 | 3.00 | 2.00 | 0.00 | 0.00 | 0.00 | 0.00 | 1.00 |
| 12 | Cidongkol | -62.41 | 1.00 | 1.00 | 2.00 | 2.00 | 0.00 | -0.08 | 1.42 | 0.07 | 1.00 |
| 13 | Batang Leutik | -43.90 | 2.00 | 1.00 | 2.00 | 2.00 | -1.25 | 0.25 | -1.23 | -0.05 | 1.00 |
| 14 | Cibadar Dua | -37.40 | 2.00 | 1.00 | 2.00 | 2.00 | 3.46 | -0.76 | -0.22 | -0.41 | 3.00 |
| 15 | Cisaga | -52.14 | 1.00 | 1.00 | 3.00 | 3.00 | -28.83 | 0.09 | -2.90 | -0.39 | 3.00 |
| 16 | Cisedari | -69.00 | 2.00 | 1.00 | 2.00 | 3.00 | -2.90 | 0.26 | -1.03 | -0.19 | 1.00 |
| 17 | Citarum | -18.40 | 2.00 | 3.00 | 1.00 | 3.00 | -76.46 | 0.08 | 1.11 | -0.16 | 2.00 |
| 18 | Cibanteng | 2.83 | 3.00 | 1.00 | 3.00 | 3.00 | 0.73 | -0.73 | 1.65 | 0.02 | 3.00 |
| 19 | Cigemari | -22.95 | 2.00 | 1.00 | 4.00 | 3.00 | 0.00 | 0.00 | 0.00 | 0.00 | 1.00 |

www.czasopisma.pan.pl          www.journals.pan.pl

PAN
POLSKA AKADEMIA NAUK

Spatial-temporal heterogeneity and driving factors of water yield services in Citarum river basin unit, West Java, Indonesia     23
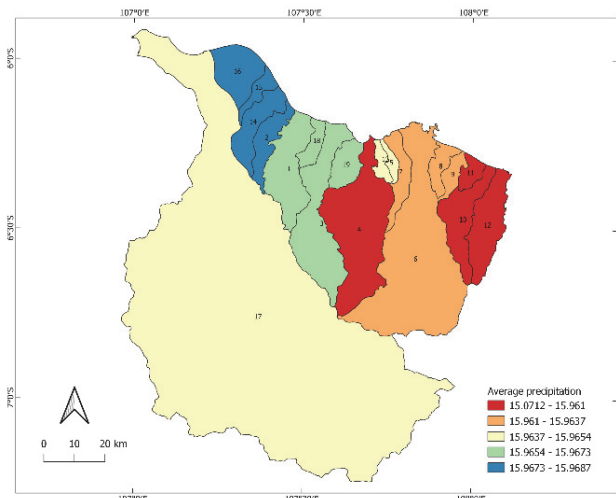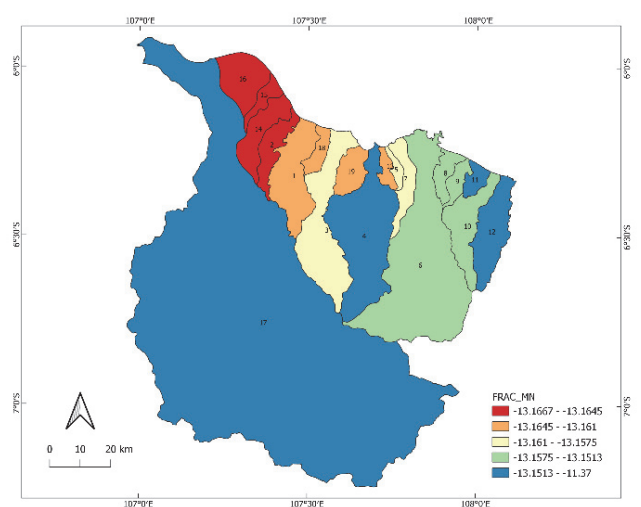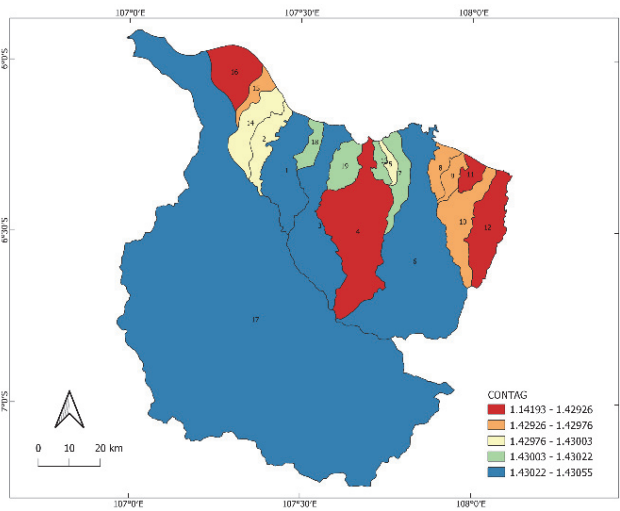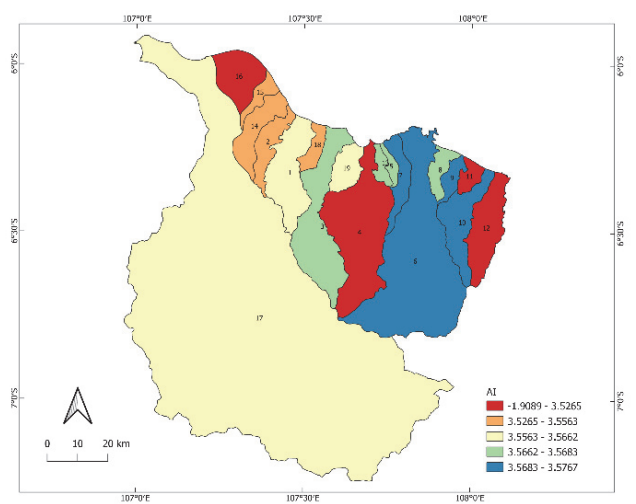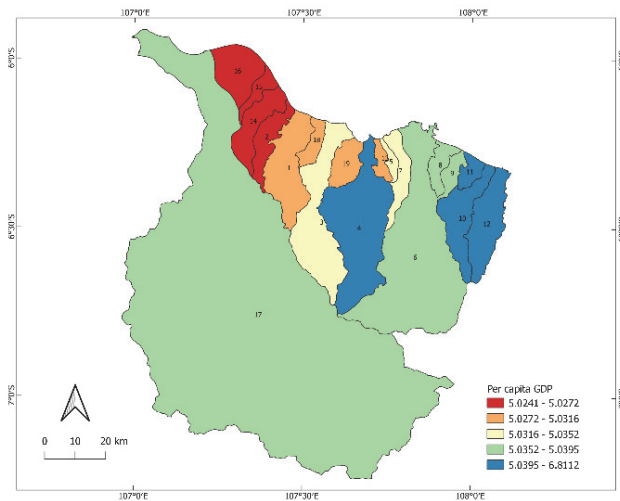


A



B
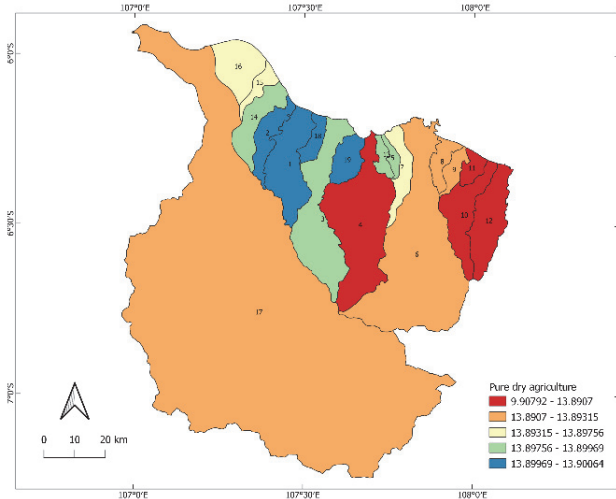


C
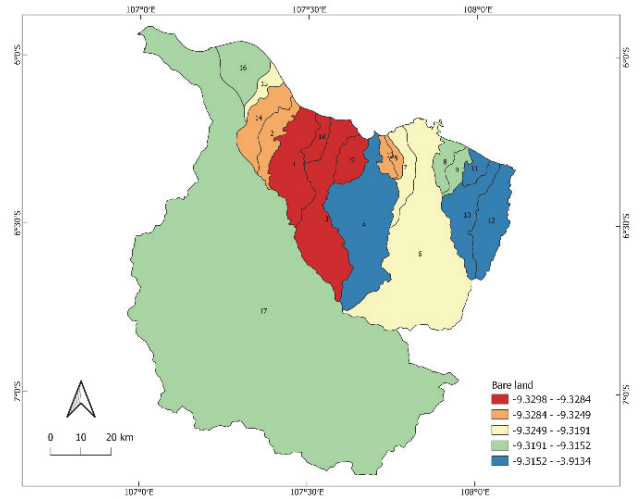


D
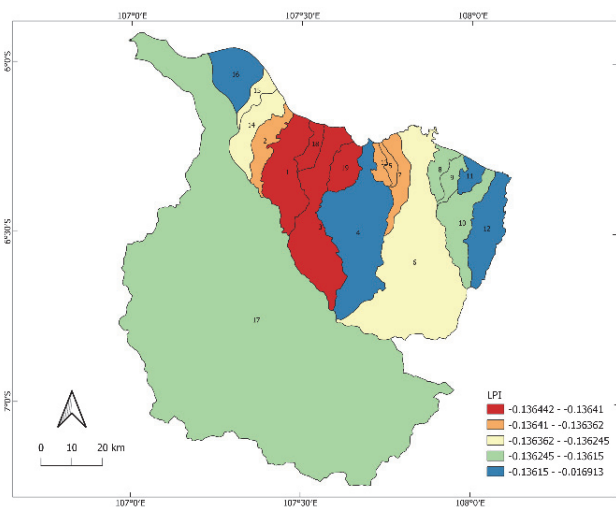


E



F

G



H



I

**Fig. S1.** Local spatial distribution of regression coefficients of GWR model (A) Average precipitation, (B) Shrub, (C) Pure Dry Agriculture, (D) Bare Land, (E) Largest Patch Index (F) Mean Fractal Dimension Index, (G) Contagion, (H) Aggregation Index, (I) Index Δ per capita GDP